

Radiation Damage in GMR Spin Valves

THESIS

Presented in Partial Fulfillment of the Requirements for the Degree Master of Science in
the Graduate School of The Ohio State University

By

Turhan Kendall Carroll

Graduate Program in Physics

The Ohio State University

2010

Master's Examination Committee:

Professor Ezekiel Johnston-Halperin, Advisor

Professor Jay Gupta

Copyright by
Turhan Kendall Carroll
2010

Abstract

The GMR effect has revolutionized the information technology industry. GMR read-out heads, MRAM and magnetic field sensors have become standard technologies of today's society, while magnetic random access memory (MRAM) is one of several applications of this effect which are in earlier stages. The presumption is that these materials are radiation hard with respect to both photons and particles, potentially indicating utility for nuclear energy and space based applications. However, few detailed studies of magnetism in GMR devices have been performed in radioactive environments. This work explores the effects of gamma ray and neutron irradiation on GMR spin valves. The sample structure used in this experiment is Py/Cu/Py/FeMn/Ge. To study the effects of radiation three probes of magnetization, VSM, MR, and MOKE, are correlated pre and post radiation. We present characterization of the devices for multiple device geometries and doses up to 50Mrad for gamma rays and a minimum fast flux of ($E_n > 0.5\text{MeV}$) of $6.3\text{E}12$ nv for neutrons, both of which are well above the failure threshold for radiation-hard semiconducting devices. We found that these devices were hard to both gamma and neutron irradiation, but that there were environmental factors that caused accelerated aging of our samples during the gamma irradiation experiment. We show follow-up studies based on these results, and future experiments that are currently in their early stages.

Dedication

This document is lovingly dedicated to my wife Nicole Carroll.

Acknowledgments

I would like to first acknowledge my Lord and Savior Jesus Christ, because without Him I would not have had the opportunity to be here. I would like to thank my advisor Ezekiel Johnston-Halperin for his patience, and support with me during my studies. I have learned so much from him about so many things, and I am grateful for that. I would also like to thank Sarah Parks, Ke Li, and Adam Hauser for being particularly supportive and helpful in the lab. You all helped me become functional in the lab and taught me indispensable skills that I will take with me forever. I would also like to thank my family for all their love and support, especially my brother Torey Boykin. I greatly appreciate all your encouragement through this time in my life. I would like to thank John Florio for your willingness to study with me, exchange ideas with me and help me prepare things when you had plenty of things you could have been doing instead. Also to two very close friends George Hoffman, and Gerald Hicks. Thank both of you for always encouraging and supporting me through all my decisions. Last but not least, Nicole Carroll, my lovely wife. I would like to thank you for so many things, too many to number here, but mostly for always supporting my decisions, being there for me no matter what, and loving me through anything I encountered while here. There is no way to express in words how much that means to me

Vita

June 2003Aviation Academy at Denbigh High School
2008.....B.S. Physics, North Carolina State
University
2008.....B.S. Applied Mathematics, North Carolina
State University
2008 to presentGraduate Teaching Associate, Department
of Physics, The Ohio State University

Fields of Study

Major Field: Physics

Table of Contents

Abstract	ii
Dedication	iii
Acknowledgments.....	iv
Vita.....	v
List of Figures	ix
Chapter 1: Introduction	1
Chapter 2: Background	3
2.1 GMR Effect	3
2.2 Exchange Bias	5
2.3 Types of Radiation Damage in Metals	7
2.3.1 Displacement of Electrons	7
2.3.2 Displacement of Atoms	8
2.3.3 Damage Cascade	8
2.3.4 Point Defects and Diffusion	10
2.4 Effects of Damage on Magnetism.....	11
Chapter 3: Sample Fabrication.....	13

3.1 Introduction	13
3.2 Sputter Deposition.....	13
3.3 Setting Exchange Bias.....	15
3.3.1 Growing Samples in Field.....	15
3.3.2 Field Cooling.....	16
Chapter 4: OSU Nuclear Reactor Lab Facilities.....	19
4.1 Introduction	19
4.2 Co-60 Gamma Irradiator	19
4.3 Nuclear Reactor.....	21
Chapter 5: Sample Characterization	23
5.1 Introduction	23
5.2 Vibrating Sample Magnetometry	23
5.3 Magnetoresistance.....	25
5.4 Magneto Optical Kerr Effect (MOKE)	26
Chapter 6: Experimental Results	30
6.1 Introduction	30
6.2 Gamma Irradiation Experimental Results.....	30
6.2.1 Conclusions for Gamma Radiation Experiment.....	42

6.3 Neutron Irradiation Experimental Results.....	42
6.3.1 Future Directions for the Neutron Radiation Experiment.....	45
References	49
Appendix A: GMR/MOKE Measurement Instructions	50
Appendix B: Analysis for GMR in Origin 8.....	62

List of Figures

Figure 1. A GMR device.....	3
Figure 2. (a) Schematic of the energy diagram for a GMR device with both magnetic layers parallel to each other. (b) Schematic of the energy diagram for a GMR device with both magnetic layers antiparallel to each other.	5
Figure 3. Spin valve device.....	6
Figure 4. (a) Sketch of the magnetization vs. magnetic field for a ferromagnetic. Where M_s is the saturation magnetization and H_c is the coercive field. (b) Sketch of the magnetization vs. magnetic field for a ferromagnetic coupled to an antiferromagnet.	7
Figure 5. (a) Displacement mean free path and total collision cross section for copper atoms moving in copper. (b) Damage caused by different types of radiation at the same incident energy and the energy scale of the recoil energy T	10
Figure 6. (a) Picture of sputter chamber at The Ohio State University in Prof. Yang's laboratory. (b) Picture inside the chamber of the while the plasma is generated.	14
Figure 7. The sample that was sputtered spin valve device used for the experiments discussed in this thesis. The Ge capping layer is there to protect the FeMn from oxidizing.	15
Figure 9. (a) Graph of pre field cooled sample taken with the vibrating sample magnetometer. (b) Graph of the post field cooled sample taken with the vibrating sample magnetometer. (c) Graph of field grown sample taken with vibrating sample magnetometer.....	17
Figure 10. (a) Graph of VSM data of the measured periodically over a month for field cooled sample. (b) Graph of the coercivity and exchange bias for time lapse data.	18

Figure 11. (a) Drawing of the side view of Co-60 Gamma Irradiator at The Ohio State University Nuclear Reactor Laboratory¹¹. (b) Co-60 Gamma Irradiator Dose Rate Curve.

..... 20

Figure 12. Diagram of decay for Co-60..... 21

Figure 13. The open pool research reactor at The Ohio State University. The blue glow comes from Cherenkov radiation in water.

..... 22

Figure 14. (a) Schematic of a vibrating sample magnetometer. (b) Graph of VSM Magnetic Moment vs. Field with examples of physical information that can be extracted (ie coercivity and exchange bias).

..... 24

Figure 15. (a) Schematic of a magnetoresistance measurement setup. (b) Graph of MR vs. Field with examples of physical information that can be extracted (ie coercivity and exchange bias, magnetoresistance)..... 26

Figure 16. (a) Schematic of a MOKE measurement setup. (b) Graph of Kerr Angle vs. Field with examples of physical information that can be extracted (ie coercivity and exchange bias).

..... 28

Figure 17. Graph of exchange bias vs. dose for field cooled and field grown samples from the (a) VSM measurement. (b) MR measurement. (c) MOKE measurement. All three graphs show there is no change in the exchange bias of the sample with the gamma irradiation of the samples.

..... 32

Figure 18. Graph of coercivity vs. dose for field cooled and field grown samples from the (a) VSM measurement. (b) MR measurement. (c) MOKE measurement. All three graphs show a nonmonotonic change in coercivity with the gamma irradiation of the samples.

..... 34

Figure 19. Graph of MR ratio vs. dose for field cooled and field grown samples from the. The MR decreases with increasing exposure time.

..... 35

Figure 20. (a) SEM image of an area of one of the samples that was unprotected during the gamma irradiations. (b) FIB cross section of the same location. (c) SEM image of an area of the sample that was covered with indium. (d) FIB cross section of the same indium covered areas.

..... 37

Figure 21. (a) EDS spectrum of the sample imaged in previous figure. We see carbon was deposited during gamma irradiation.

..... 38

Figure 22. New sample structure used for the followup gamma irradiation study.

..... 40

Figure 23. MR results for the followup experiment. MR completely gone after just 2 days of exposure

..... 41

Figure 24. (a) SEM images of the sample after 2 days of exposure show the same surface damage it took a month to see in the previous study. (b) Before irradiation the glass vials in which the samples were irradiated were clear. (c) After 1 day of exposure, there is a very strong browning and aging effect that takes place.

..... 41

Figure 25. Graph of the coercivity vs. fast neutron flux for both the MR and MOKE measurements. The blue line is the MR measurement and the brown line is the MOKE measurement.

..... 43

Figure 26. Graph of the exchange bias vs. fast neutron flux for both the MR and MOKE measurements. The blue line is the MR measurement and the brown line is the MOKE measurement.	44
Figure 27. Graph of the MR Ratio vs. fast neutron flux.	45
Figure 28. Low Temperature system for the neutron experiment.	47
Figure 29. Pasting Sample onto Sample stick and attaching indium press contacts.	52
Figure 30. Sample wired on the stick.....	53
Figure 31. Sample inside magnet.....	54
Figure 32. GMR setup and breakout box.	55
Figure 33. GMR electronics.....	56
Figure 34. Kepco power supply and GMR lockin.	57
Figure 35. Schematic, and picture of MOKE setup.....	59
Figure 36. : Laser and Polarizers on MOKE setup.	60
Figure 37. MOKE electronics.	61

Chapter 1: Introduction

Giant magnetoresistance (GMR) was discovered by Peter Grünberg and Albert Fert independently, in 1988. It demonstrated a large change in resistance as a function of magnetic field, magnetoresistance (MR), in devices that consisted of magnetic multilayer stacks. These systems found a change in MR to be 4% in a trilayer system of Fe/Cr/Fe at room temperature and 50% in a stack that alternated Fe and Cr in 60 layers at 4.2 K¹⁻². This discovery was much larger than what anyone had seen in an MR signal before. Grünberg and Fert received the Noble Prize in Physics in 2007 for their discovery of GMR³.

Giant Magnetoresistance (GMR) is an effect whose discovery is one of the most exciting milestones in solid state physics. This is due to the fact that its discovery gave insights to new combinations of materials with novel properties that did not fit into any category that had been previously studied. GMR has already been established as a unique phenomenon that combines properties of metals and magnetic materials to another new class of materials. It has already found several technical applications and it is widely being used in industry, primarily as the basic component of read heads in magnetic recording⁴.

From the discovery of GMR, a new field of physics has been emerging, that of spintronics or spin electronics. The name is self-explanatory: the physical property that is

the principal focus in these materials is the spin of the electrons. Although the field of spintronics is new, it is promising in the area of pure science because it is rich in physics and in applied physics because it offers the opportunity for the creation of novel devices such as the spin transistor.

Chapter 2: Background

2.1 GMR Effect

A GMR device generally consists of two ferromagnetic thin films with a nonmagnetic metal sandwiched in between (Figure 1). The nonmagnetic spacer layer's material (usually Cu or Cr), and thickness must be chosen to meet several criteria: 1) the spacer must have good electrical and spin conduction across the whole layer, 2) it must be thin enough to have good spin transport across the spacer, while at the same time being thick enough to prevent the magnetic layers from strongly coupling to each other³. In figure 2 a sketch of the magnetic configuration for the FM/NM/FM (ferromagnetic/non magnetic/ferromagnetic) multilayer is made together with the corresponding energy diagram for the two ferromagnetic layers (FM). In Figure 2a the magnetizations of the two FM layers will be parallel . In Figure 2b the two FM layers are magnetized in such a way that they have opposite magnetization directions.

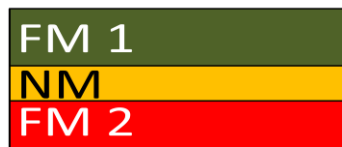


Figure 1: A GMR device

An electrical current is now sent through the system for both configurations. In each schematic in Figure 2, the current is initially made up of an equal number of up and

down spins. In Figure 2a when the electrons reach the ferromagnet, the ones with down spins cannot be easily transmitted through because the Fermi energy is too low to include the down spins. This causes the down spins to be heavily scattered through this FM layer. The same thing is true when it reaches the second layer so only a net up spin will be transmitted through the parallel device easily, while the spin down spins will be scattered.

However in Figure 2b now it is in the antiparallel state, so when the initial current passes through the first layer, only a net down spins are transmitted, while the net up spins are scattered. When it reaches the second layer, the Fermi energy will only allow the up spins to be transmitted easily. This leads to an increase in resistance since neither the up or down spins can be transmitted through the device, so we would call this configuration the high resistance configuration for the device. In the parallel state, on the other hand one of the two spins will easily pass through the device, so we would refer to it as the low resistance configuration of the device. The spin dependent scattering described here is the primary cause of GMR.

It should be noted that when an electron leaves the first iron layer and enters the non-magnetic metal there will be additional scattering processes giving rise to extra resistance. Since the spin up and spin down particles have different density of states at the Fermi, the resistance not only within the FM layers, but also that originating from the FM/NM interface will be different for the two spins. Inside the NM layer the up and down spins will experience the same resistance, but generally this is low compared to those in the FM layers and FM/NM interfaces and can here be neglected⁵.

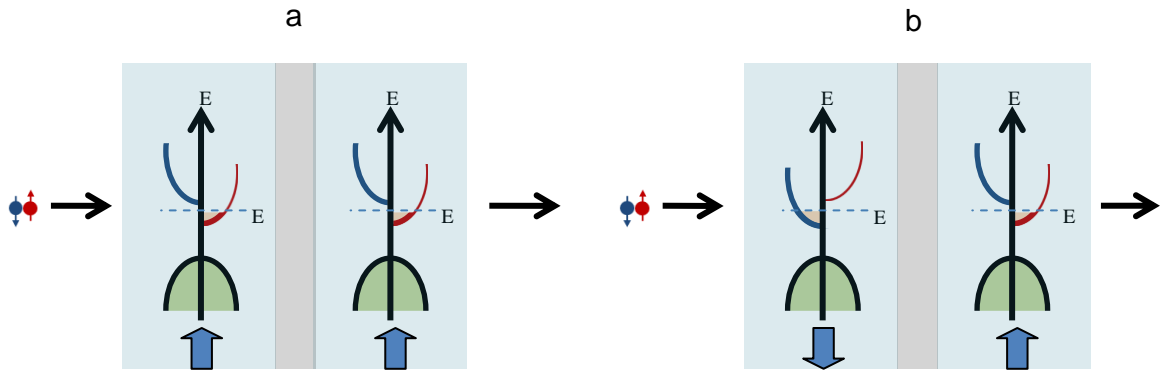


Figure 2: (a) Schematic of the energy diagram for a GMR device with both magnetic layers parallel to each other. (b) Schematic of the energy diagram for a GMR device with both magnetic layers antiparallel to each other.

2.2 Exchange Bias

The GMR devices discussed in this thesis are called spin valve devices. A spin valve has the FM/NM/FM sandwich discussed in last section, but one of the FM layers is “pinned” by coupling it to an antiferromagnet (AFM) as shown in Figure 3. Whenever an AFM is coupled to a FM this exchange biases the FM.

Exchange bias is defined as the unidirectional pinning of a ferromagnetic layer by an adjacent AFM. Ordinary ferromagnetic materials have not one but two equally favored magnetic directions, which are collinear and lie along the so-called "easy axis". Thus two equally stable magnetization directions have the same energy, and the same magnitude of an external field is required to rotate the magnetization by 180° from one easy direction to the other. As shown on the left side of Figure 4, the magnetization loop is therefore symmetric about zero field.



Figure 3: Spin valve device

When a ferromagnet is simply grown on top of an antiferromagnet the exchange coupling between the two systems only leads to an increased coercivity of the ferromagnet. This is usually attributed to the increased coercivity of “interfacial spins” which need to be dragged around by the external field⁶⁻⁸. However, the ferromagnetic hysteresis loop is still symmetric, indicating two equivalent easy directions. If, on the other hand, the AFM-FM system is grown in a magnetic field or after growth is annealed in a magnetic field to temperatures above the AFM Néel temperature, the hysteresis loop is shifted from zero (Figure 4 right) and can even become asymmetric. This unidirectional shift is called exchange bias and reflects the fact that there is now a preferred easy magnetization direction for the FM. The magnetization \mathbf{M} of the ferromagnet is pinned by the antiferromagnet into this direction.

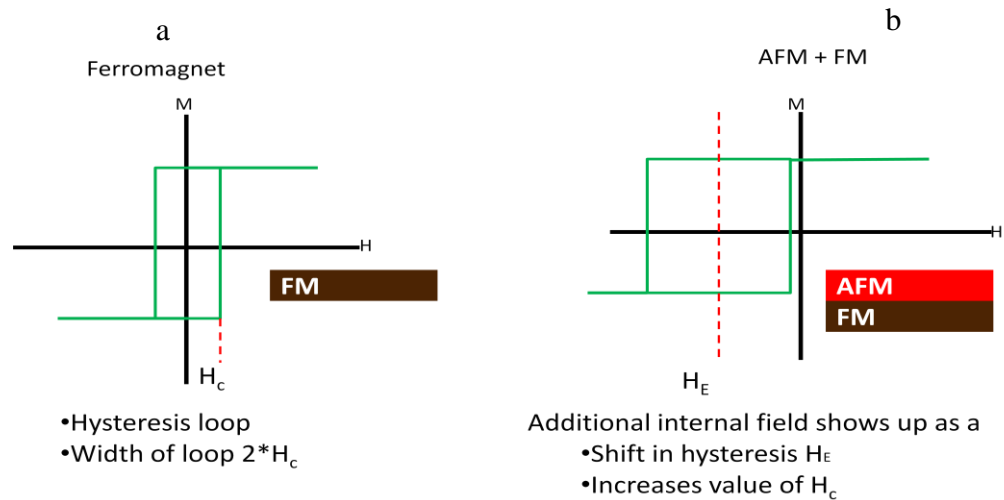


Figure 4: (a) Sketch of the magnetization vs. magnetic field for a ferromagnetic. Where M_s is the saturation magnetization and H_c is the coercive field. (b) Sketch of the magnetization vs. magnetic field for a ferromagnetic coupled to an antiferromagnet.

2.3 Types of Radiation Damage in Metals

Here we describe several types of damage that radiation can cause in metals. These types of damage are mainly structural deformations. It is not clear, however that structural damage causes changes in the magnetic properties of GMR spin valves.

2.3.1 Displacement of Electrons

The main damage that can occur during gamma irradiation are electron displacements. As the name indicates, this occurs when an incident gamma ray causes an electron to leave its orbital. If the electron has enough momentum, it can cause an avalanche, or cascade of electrons from the initial event. Since we are working with metals, and the electrons are free to move in the material, this electron excitation should

not cause significant amounts of damage because the electrons have enough mobility to recombine quickly¹⁰.

This electron displacement effect could however become important in the antiferromagnetic layer if it were to enough electrons were displaced by either by a damage cascade, or by the gamma rays themselves. If this were to happen, it would cause changes to the exchange bias, and to the coercivity of the exchange biased layer. In order for this to happen there would have to be a lot of interaction between the gamma rays and the electrons in the antiferromagnet.

2.3.2 Displacements of Atoms

As mentioned above, one would not expect gamma rays to cause significant damage in metals except in extreme circumstances, since they mainly cause electron displacements. Neutrons, on the other hand can cause displacement of atoms from a lattice space¹¹. The process of a neutron displacing an atom occurs in six steps. First the neutron is incident on an atom that is sitting on a lattice. The neutron then transfers some its kinetic energy to the lattice atom. This begins the displacement of the atom. The atom is then displaced from its lattice site. Next the atom moves through the lattice bumping against more atoms. This creates a damage cascade. Finally, the initially displaced atom comes to rest and becomes an interstitial¹². It's clear from this process that the initial displacement causes the damage.

2.3.3 Damage Cascade

In theory damage cascade could be caused by electron displacements (from gamma rays for example), or from displacements in atoms. Since this thesis covers only

damage in metals, we will restrict our discussion in this section to damage cascades caused by the later, because damage caused by electron displacements should be negligible in metals. The amount of damage caused by the initially hit atom is dependent on the amount energy the this atom has after the initial collision. In order for the atom to move about the lattice, it must have an energy greater than the displacement energy of that particular atom. If it does, then the cascade for a given particle depends on the collision cross section and mean free path of the atoms in the lattice. So if there is a short mean free path and a large collision cross section, then there will be a large amount of damage to the sample. This can be seen for copper in Figure 5a below. The largest number of collisions occur in copper when the energy of the initially hit atom is between 50 and 100keV. This is where the collision cross section is the largest and the mean free path is the smallest in copper¹³.

Figure 5b shows the damage cascade for different types of particles. Two cases are of interest for this thesis: electrons, and neutrons since those are the two types of particles that could cause damage in our samples. For electrons, if the gamma irradiation were to produce electron that had energy high enough it could create a vacancy (denoted by the open square in Fig. 5b) and an interstitial (denoted by the black circle in Fig. 5b). However, it is not likely to cause a significant amount of damage because each electron is only likely to create a single vacancy- interstitial pair.

A neutron with high enough energy, causes a cluster of vacancy- interstitial pairs when it collides with an atom in the lattice (Figure 5b). The neutron is the most efficient

at transferring its energy to the initially hit atom, which causes point and cluster defects in the lattice¹².

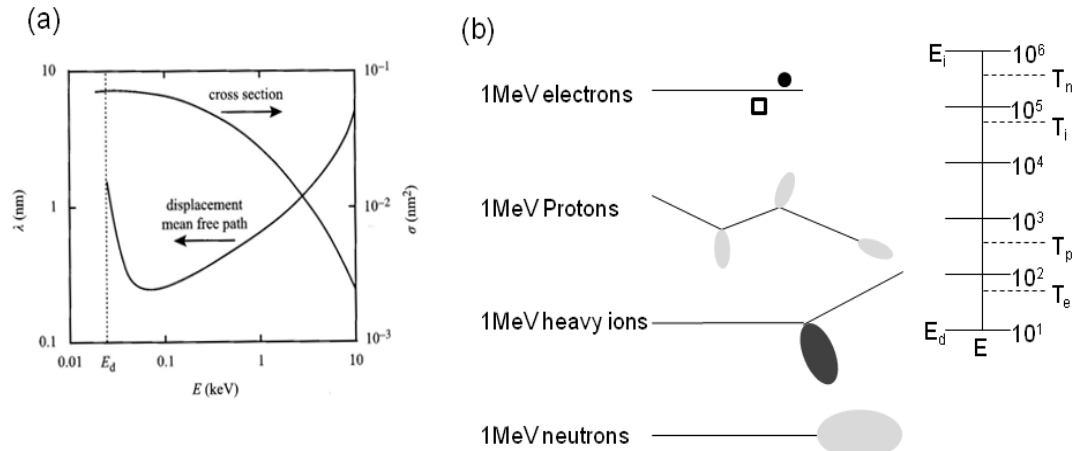


Figure 5: (a) Displacement mean free path and total collision cross section for copper atoms moving in copper. (b) Damage caused by different types of radiation at the same incident energy and the energy scale of the recoil energy T ¹².

2.3.4 Point Defects and Diffusion

There are two types of defects caused by irradiation. First are called interstitials. An interstitial is an atom that is not on a lattice site (ie the atom occupies a location where there is usually not an atom present). It is possible to have multiple interstitials close to each other. When this occurs the interstitials can bind together and have a high binding energy on the order of 1eV. Interstitials have a high mobility in the lattice because they have a high formation energy, large relaxation volume, and a low migration energy¹².

The second point defect is a vacancy which is a lattice site that is actually missing an atom. Like interstitials, multiple vacancies can form near each other, but in this case the binding energies are much smaller than those of interstitials, on order of about 0.1eV.

Vacancies have low mobility compared to interstitial atoms also, which means that they are less likely to move around the lattice¹².

Since interstitial atoms are very mobile, it is possible at room temperature for the lattice to anneal itself. This is less likely to happen if the initially displaced atom has enough energy to move it far from the vacancy that is created when it moves. In order for this to occur, the reactor must have many fast neutrons, with energies greater than 0.05eV^{12} . Fast neutrons are the highest energy neutrons in a reactor and are most likely to cause structural damage during an irradiation.

2.4 Effects of Damage on Magnetism

The effects that the types of damage mentioned above will have on magneto transport are dependent upon the type of irradiation the sample experience, and the type of damage inflicted during the irradiation. For example, gamma irradiation would likely only cause electron displacements. In order for these displacements to affect the magneto transport in our samples, enough electrons would have to be displaced to cause the material to lose its magnetic ordering. Realistically, however this is unlikely to impact the ferromagnetic layers because the electrons will reorder when the sample is placed in a magnetic field, which would be the case for all of the characterization that we do. Another effect that we may observe during a gamma irradiation is if enough disorder is produced in the antiferromagnetic layer. If enough electrons are displaced in this layer, it is possible that they would not reorder properly which would cause changes to the exchange bias and coercivity of the top ferromagnetic layer.

During neutron irradiations, it is possible to move atoms in the sample. This could lead to domain wall formation, which could in turn impact the coercivity, exchange bias, or magnetoresistance of the sample depending on which layer(s) have displaced atoms¹¹. If the atoms were predominantly knocked out in the antiferromagnetic layer but still remained in the antiferromagnetic layer, then it would cause changes to the exchange bias and the coercivity. If atoms were knocked out of the antiferromagnetic layer and were knocked into the ferromagnetic layer then it would be expected to see all three measurements changed since it would place an impurity in the ferromagnetic layer. If it were just atoms in the ferromagnetic layer that were moved it would probably mostly be seen in the MR ratio measurement. If atoms are knocked out of place, there need not necessarily be many atoms moved to see a noticeable effect in the sample.

Chapter 3: Sample Fabrication

3.1 Introduction

Several steps must be taken to fabricate the sample and prepare it for irradiation. First off the materials are sputter deposited onto the sample. Next the sample is cut to the desired size. Finally the exchange must be established in the samples. The last step can be accomplished either by field cooling the sample, or growing the sample in the presence of a magnetic field.

3.2 Sputter Deposition

Our samples are grown at The Ohio State University in the magnetron sputtering system designed and built by the Yang group in the physics department. The chamber is used for growth of thin film samples. It is kept in ultra high vacuum with typical conditions of around 5×10^{-10} torr. The sputtering process is a physical vapor deposition used to deposit material on a substrate. To accomplish this deposition a high purity argon gas is ionized and then bombarded on the positively biased target. This causes a high energy plasma to be created above the target. The substrate is placed above the target in the plasma region. The material being sputtered collects on the substrate and cools forming a uniform layer of material. Calibration of how fast to sputter the material is done when the target are first put in the chamber by students in the Yang group. Figure 6a is a picture of the sputtering chamber; the samples are loaded through a load lock seen in

the left side of the picture in to the main chamber. Figure 6b is a picture of the target, plasma and sample during a deposition.

All of the targets in the chamber are preloaded in the chamber so vacuum is never broken until the final layer is deposited. A load lock is used to place the substrate in the chamber. For the radiation samples the layers deposited on the substrate are Py (Ni₈₀Fe₂₀) 100Å, Cu 61Å, Py 100Å, Fe₅₀Mn₅₀ 200Å, Ge 100Å grown on top of 1 inch by 1 inch Si wafer with 3000Å of thermally grown oxide Figure 7.

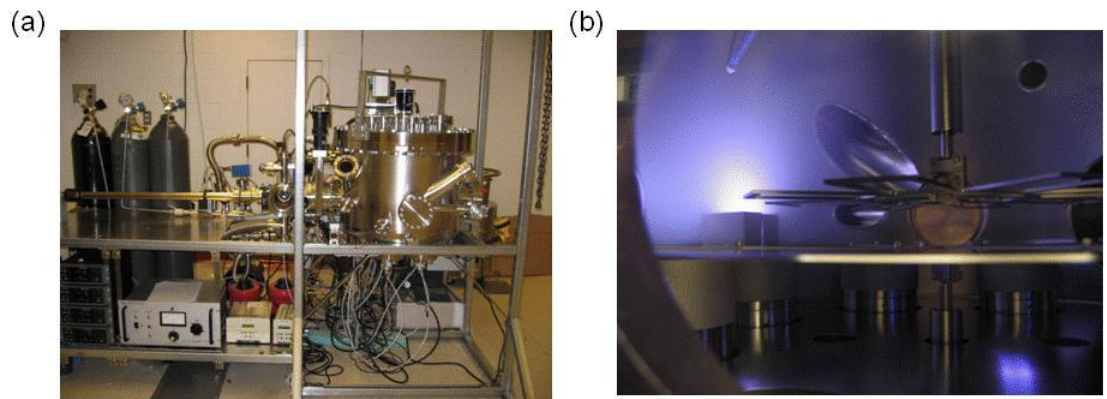


Figure 6: (a) Picture of sputter chamber at The Ohio State University in Prof. Yang's laboratory. (b) Picture inside the chamber of the while the plasma is generated.

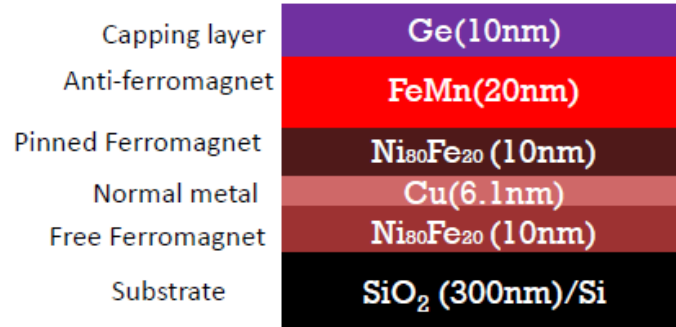


Figure 7: The sample that was sputtered spin valve device used for the experiments discussed in this thesis. The Ge capping layer is there to protect the FeMn from oxidizing.

3.3 Setting up Exchange Bias

When an antiferromagnet comes in contact with a ferromagnet, an exchange bias can be set up at the interface between the two which will cause the FM layer to switch at a different value than it would had it not been exchange biased. There are two ways to set up exchange bias in our samples. Both order the FeMn layer in its AFM state. Once the AFM is ordered, the exchange bias is set.

3.3.1 Growing Samples in Field

One of the methods we used to grow samples for this experiment was to grow the samples in field. This just simply means that the materials were sputtered onto the substrate in the presence of a magnetic field. The field was established by putting two magnets on the platform that the substrate rested on, and at opposite ends of the substrate (see Figure 8). This causes the FeMn layer to order as the sample is grown. When the

magnetization is measured right out of the chamber, it has a profile similar to that of Figure 9b.

3.3.2 Field Cooling

Field cooling is the other method we used to set up exchange bias in our samples. The field cooling process we used for our samples involves several steps. First once the sample is sputter deposited and cut to size, we placed the sample between the poles of an electromagnet. The temperature of the sample is then raised to the Neel temperature, which is the ordering temperature of the AFM (420K in the case of FeMn)¹⁴. It should be noted that whenever field cooling is performed, it is important that the materials are chosen so that the Neel temperature of the AFM is lower than the Curie temperature of the FM to avoid loss of FM ordering. Once the temperature is stable at 420K, a large magnetic field is applied to the sample, for our samples we applied a 1.5T field. Then, with the field still applied, the temperature of the sample is lowered back down to room temperature, which takes roughly 30 minutes. Once the sample is cooled to room temperature, the field is lowered back to 0T. Plots of the magnetic moment of a sample both before and after it was field cooled is shown in Figure 9. Figure 9a is the sample before it is field cooled. Notice that in this graph it is impossible to resolve two independent permalloy switches. It is clear, however that there is some distortion toward the bottom of the magnetization curve in Fig. 9a. This distortion is in the same location that the exchange biased switch occurs in Figure 9b, which would tell us that the location on the sample where distortion is the top permalloy layer which is coupled to the unordered FeMn layer. Figure 9b shows the magnetization curve after the sample was

field cooled. The switch due to the unbiased permalloy layer occurs at -1G and 0.9G. The switch due to the permalloy layer that is coupled to the FeMn layer occurs at -17G and -7G.

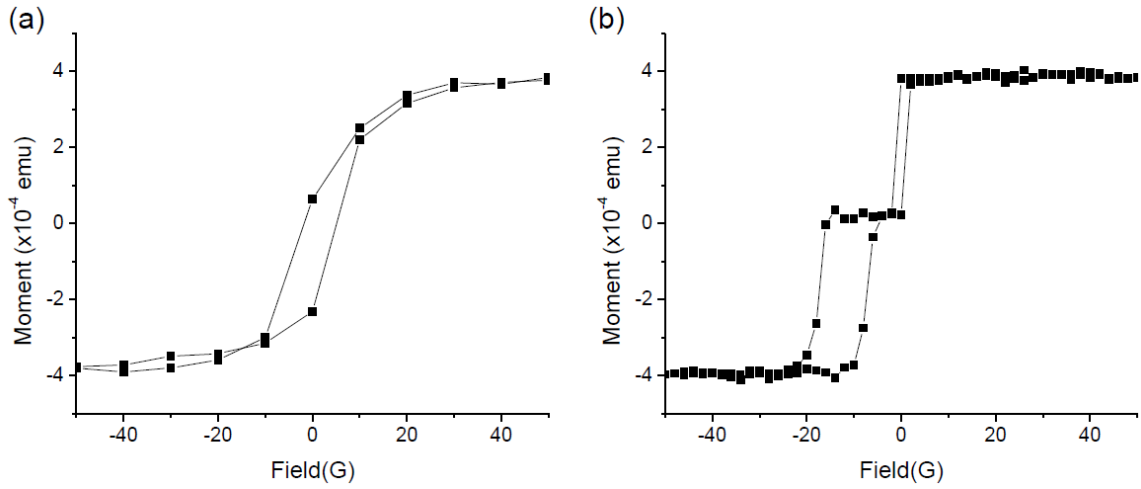


Figure 9: (a) Graph of pre field cooled sample taken with the vibrating sample magnetometer. (b) Graph of the post field cooled sample taken with the vibrating sample magnetometer.

There are several advantages and disadvantages for each growth method. The advantages of field cooling are that it has a relatively high magnetoresistance ratio, roughly 1.5%. The disadvantages however are two-fold. First off the coercivity and exchange bias are not stable. Figure 10 shows both the magnetization curves taken over a period of one month for one sample, and the coercivity and exchange bias for the same sample over that period of time. It is clear from this data that once a sample is field cooled the magnetic properties of the sample must relax over a period of one month.

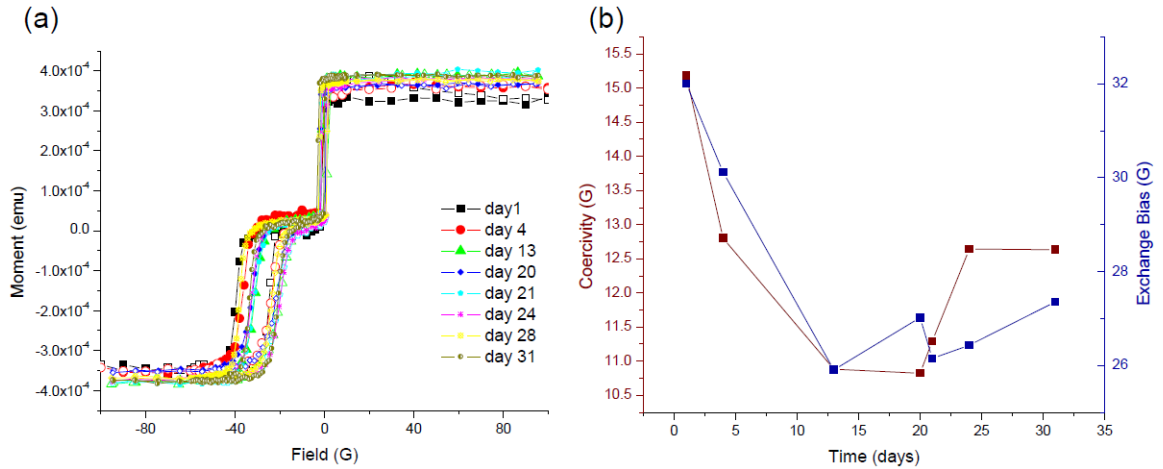


Figure 10: (a) Graph of VSM data of the measured periodically over a month for field cooled sample. (b) Graph of the coercivity and exchange bias for time lapse data.

There are essentially two advantages to field growing samples as opposed to field cooling them. First off, the sample preparation is easier and less time consuming, because there is no extra work needed to set up the exchange bias once the sample is grown. Secondly, the coercivity and exchange bias are stable over time, within the accuracy of our measurements, so there is no relaxation period over which we expect to see drifts in the exchange bias and coercivity. The major disadvantage of field grown samples is that they have much smaller MR ratios than field cooled samples. The MR ratio is large enough for the measurements taken for this thesis though.

Chapter 4: OSU Nuclear Reactor Lab Facilities

4.1 Introduction

The Ohio State University Nuclear Reactor Lab is a research reactor facility. It has been in operation since 1961, and is used for various research, instructional, and service activities. There are various types of research conducted in these facilities including neutron activation analysis (NAA), radiation-damage evaluation for electronic components and for other materials, evaluation of neutron and radiation sensitive detectors, isotope production, and biomedical experiments¹⁵. The experiments presented in this thesis use two of the three reactors at the NRL, the Co-60 gamma irradiator, and the reactor for neutron irradiations.

4.2 Co-60 Gamma Irradiator

The ^{60}Co gamma irradiator is shown in the schematic in Figure 11 (a). This design has an elevator that allows the sample to be taken in and out of the ^{60}Co irradiator. The tube is 6 inches in diameter but only has a 4 inch usable area in the tube because of the elevator. The dose amount at the OSU nuclear reactor is seen in Figure 11 (b)¹⁵. The ^{60}Co irradiator has its peak dose at about 7 inches from the bottom of the elevator. This is because the source is not at the bottom of the elevator but instead it is located several inches up. The ^{60}Co surrounds the elevator so the sample is irradiated from a 4π solid angle.

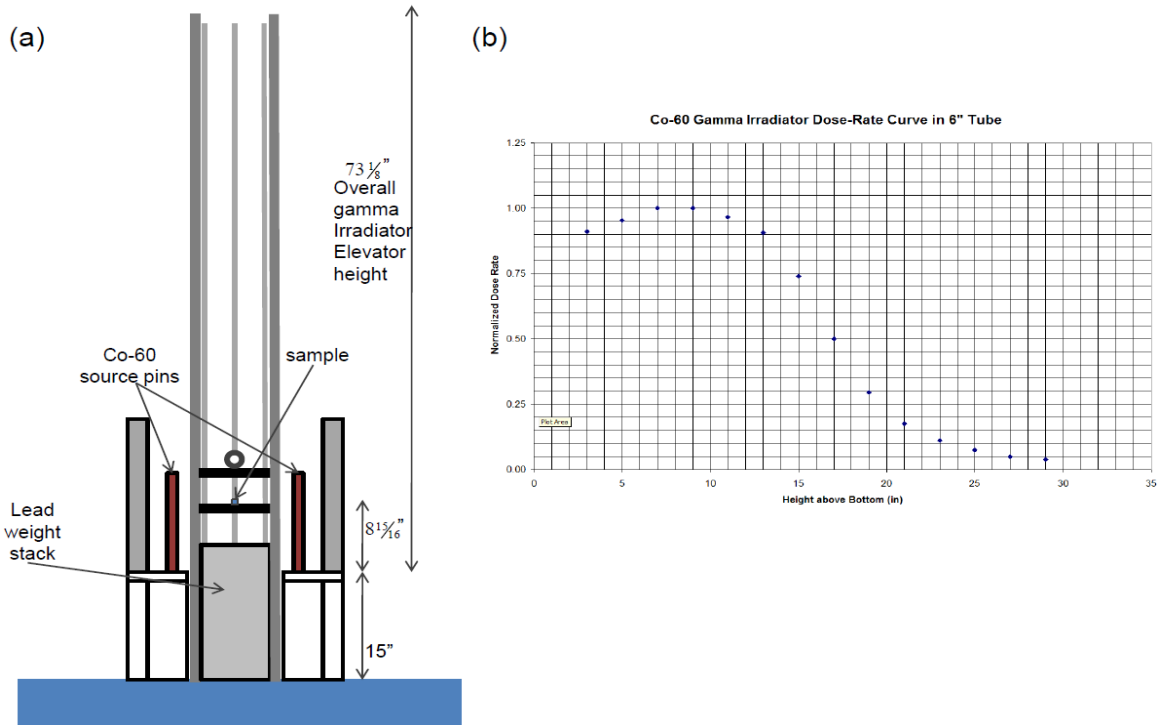


Figure 11: (a) Drawing of the side view of Co-60 Gamma Irradiator at The Ohio State University Nuclear Reactor Laboratory¹¹. (b) Co-60 Gamma Irradiator Dose Rate Curve¹⁵.

In order to create the ^{60}Co source, cobalt pins are dipped in the neutron reactor which forms the commonly found isotope of ^{59}Co to ^{60}Co . ^{60}Co has a reasonable half life of 5.271 years¹⁵. The drawing of the decay of ^{60}Co is shown in Figure 12. The ^{60}Co first decays by a β^- emission with an energy of 0.315MeV to become $^{60}_{28}\text{Ni}$. Then it decays by two gamma emissions the first at 1.1732MeV and the second at 1.3325MeV.

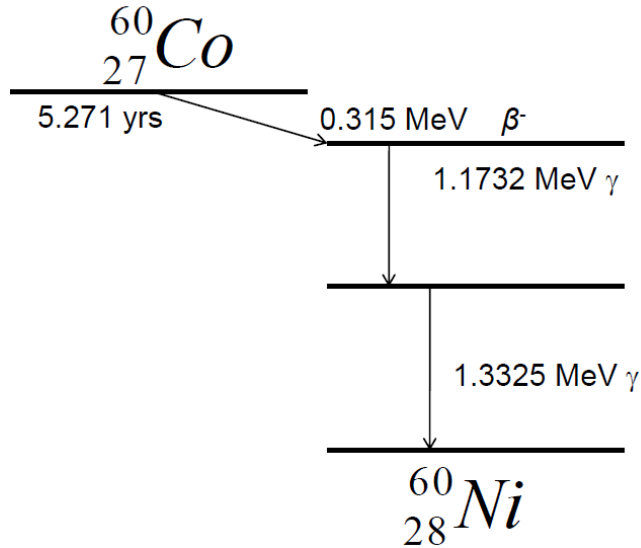


Figure 12: Diagram of decay for Co-60¹⁶.

4.3 Neutron Reactor

The neutron reactor is an open pool-type reactor, seen in the picture in Figure 13, which provides the cooling for the reactor. The reactor fuel source is 19.5% enriched U_3Si_2 and operates at a continuously variable thermal power with a maximum power output of 500 kilowatts. The average thermal neutron flux is 5×10^{12} neutrons / cm^2/s at full power. There are several access points to the areas with neutron irradiation, however only two will be used for this project, beam port 1 and the pneumatic transfer (rabbit). The beam port 1 has access through a porthole into a 6 inch diameter tube that is in the reactor pool. This beam port has a maximum total flux of 7.8×10^{12} n/ cm^2/s and maximum thermal flux of 4.5×10^{12} n/ cm^2/s . Beam port 1 has the capability to make temperature measurements at the same time the sample is in the reactor. This is useful

because the samples are known to degrade with temperature. When running a sample in beam port 1 it is only possible to utilize 20% of the full power of the reactor. The rabbit port allows easy access to the samples, however cannot make temperature measurements because it is a closed system. This port however allows the reactor to be easily run at 90% full power of the reactor. The rabbit system has a two inch diameter tube that carries the sample to the area of irradiation. The maximum total flux is 2.7×10^{12} n/cm²/s with a maximum thermal flux of 1.8×10^{12} n/cm²/s is available in the rabbit port.



Figure 13: The open pool research reactor at The Ohio State University. The blue glow comes from Cherenkov radiation in water.

Chapter 5: Sample Characterization

5.1 Introduction

Our laboratory had access to several different tools which can be used for magnetic characterization. For the data presented in this thesis three different characterization techniques were used. All samples were measured using each technique making it possible to see if any part of magnetic properties was affected more than another by irradiating them. The characterization techniques used were vibrating sample magnetometry (VSM), magnetoresistance (MR), and magneto optical Kerr effect magnetometry (MOKE).

5.2 Vibrating Sample Magnetometry

The VSM is shown in the drawing in Figure 14a. The VSM consists of a large electromagnet, pickup coils and an oscillator. The oscillator physically vibrates the sample at a frequency of 80 Hz. When a magnetic sample is attached to the sample rod, this vibration will induce an emf in the pickup coils according to Faraday's law, where a changing magnetic field through a coil will induce an emf. Then the electromagnet is swept between a given set of field values and at each field value, the voltage is measured. The induced voltage in the pickup coil is proportional to the sample's magnetic moment, but does not depend on the strength of the applied magnetic field. This will give a hysteresis curve as seen in Figure 14b.

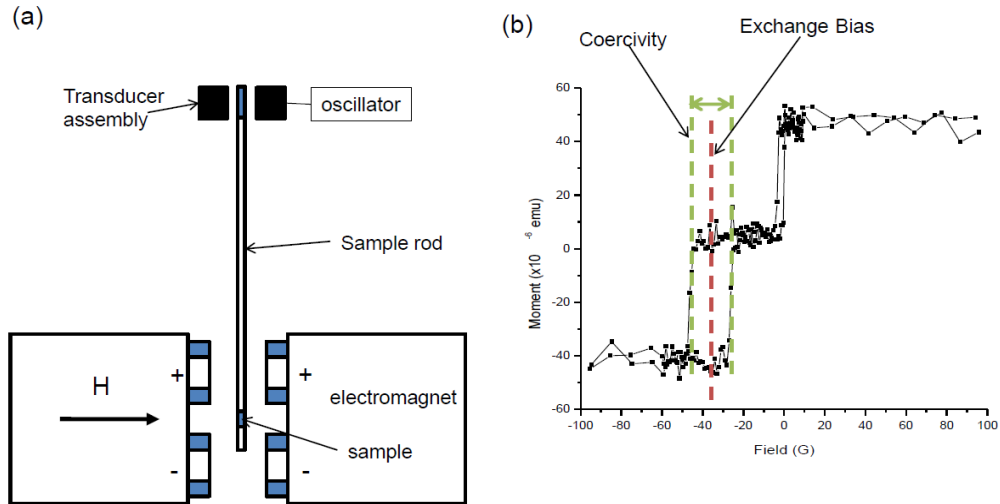


Figure 14: (a) Schematic of a vibrating sample magnetometer. (b) Graph of VSM Magnetic Moment vs. Field with examples of physical information that can be extracted (ie coercivity and exchange bias).

From the hysteresis curve shown in Figure 14b several pieces of important information can be gathered. First off notice that there are two distinct transitions in magnetization, denoted by the two loops in the graph. One of the loops is centered around zero, and the other is shifted from zero by some amount. The transition centered around zero corresponds to changes in the magnetization of the bottom-most permalloy layer. The shifted, and wider loop corresponds to changes in magnetization for the top permalloy layer that is coupled with the FeMn.

As denoted in Figure 14b the width of the two loops on this curve is known as the *coercivity* of the magnetic layer that it corresponds to. Coercivity is a measure of how much energy it takes to switch the direction of magnetization of a ferromagnet. Notice it takes more energy to switch the exchange coupled layer, then it does to switch the

uncoupled permalloy layer, just as one may expect. The shift off zero denoted in Figure 14 is the physical manifestation of the *exchange bias* discussed earlier in this thesis. It should also be noted that even though it was not considered relevant to the experiments discussed here, it is also possible to measure the magnetic moment from VSM data, and the particular setup we used for this experiment is able to measure the magnetic moment to an accuracy 1×10^{-7} emu.

5.3 Magnetoresistance

The next characterization measurement that we perform is called a magnetoresistance measurement. This measurement measures the resistance of the sample while the field is swept. There are several parameters that can be observed from a MR measurement. Like the VSM measurement, it is possible to monitor the coercivity and exchange bias of the sample, but with MR it is also possible to calculate the *MR ratio* since $MR \text{ ratio} = \frac{R_{peak} - R_{base}}{R_{base}}$ (see Figure 15b).

The magnetoresistance (MR) measurement set up is shown in the drawing in Figure 15a. This set up measures the differential resistance of the sample while the field is swept. This is done using a one Tesla magnet from while measuring the differential resistance of the sample using a DC/AC source meter with a lock-in. The sample is wired to copper wires using pressed indium contacts and is then placed on a sample rod and wired to the sample rod.

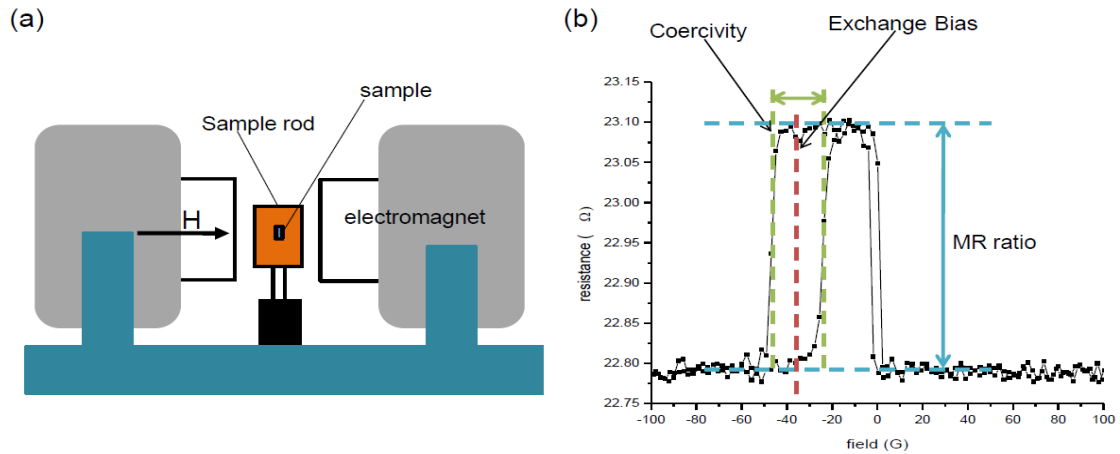


Figure 15: (a) Schematic of a magnetoresistance measurement setup. (b) Graph of MR vs. Field with examples of physical information that can be extracted (ie coercivity and exchange bias, magnetoresistance).

5.4 Magneto Optical Kerr Effect (MOKE)

The third characterization technique we used is MOKE. Magneto Optical Kerr Effect (MOKE) uses light to probe information about the samples magnetization. To do this polarized light is incident on the magnetic samples surface. The polarization of the light interacts with the magnetization of the sample and the polarization of the light and the reflectivity of the light can be changed. This change can be measured. How the polarization of the light interacts with the sample depends on the magnetization of the sample where the laser light is incident on the sample, so if the magnetic field is swept over fields such that the magnetization of the sample changes, then the reflected polarized light will also change with the magnetic field because of the interaction with the sample.

The optical equipment need to run this experiment is helium neon (HeNe) laser, used along with a chopper, two polarizers, two focusing lenses and a photo diode as is shown in Figure 16a. The light first passes through the first polarizer ensuring the light is all vertically polarized. The light is then passed through an optical chopper set at its maximum frequency of 1000 Hz to modulate the laser signal. It then passes through a lens that focuses the light on the sample. The light is next incident on the sample. The light then passes through a second focusing lens, a second polarizer that is set to minimize the light passing through it. The photodiode then converts the light signal intensity into a current. Then to amplify the signal it passed through a current amplifier which amplifies the signal and converts the signal to voltage and is then feed into the lock-in.

Figure 16b is the plot of the Kerr angle vs. the magnetic field. Since this is also a measurement of the magnetization, it is best compared with Figure 14b which is the data from the VSM. The switching fields are consistent with the two switches in the magnetic moment data seen and hysteresis in both curves. However unlike the VSM magnetization data, the two hysteresis curves are not evenly spaced along the y-axis. This is caused by the penetration depth of the laser, the deeper the laser has to penetrate in to the sample to interact with the material the weaker the signal will be. Since the exchange biased permalloy layer is closer to the surface it dominates the signal. However the penetration depth of the laser is deep enough to be able to measure the permalloy layer alone.

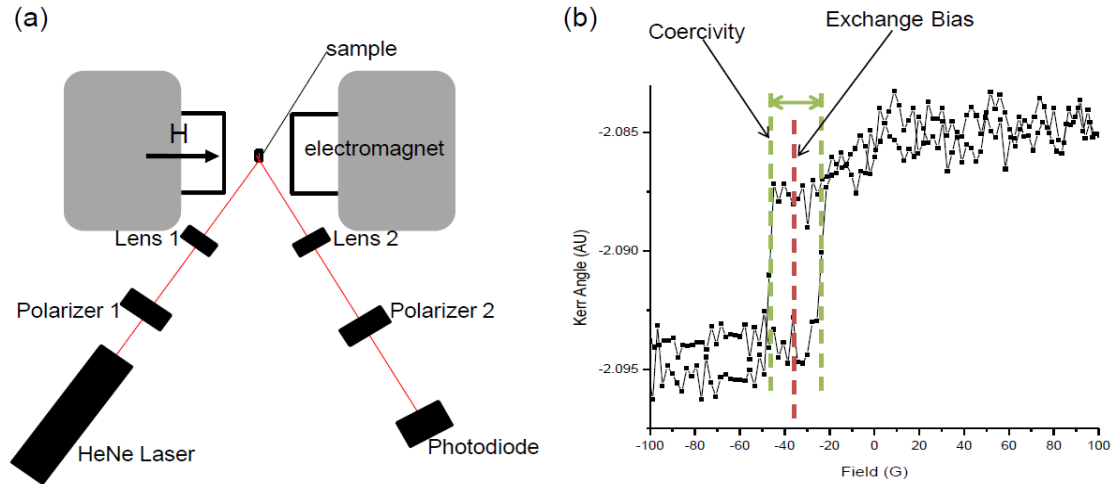


Figure 16: (a) Schematic of a MOKE measurement setup. (b) Graph of Kerr Angle vs. Field with examples of physical information that can be extracted (ie coercivity and exchange bias).

From this graph it is again possible to measure the coercivity in green and the exchange bias in red. This should be measured in the same fashion that the coercivity and exchange bias are measured in the VSM data.

The resolution of this measurement is strongly dependent on several factors. The first is the same as the MR data where it is resolution limited to 1 G by the instrumentation. However, since this is an optical measurement that is dependent on the surface of the sample remaining clean and smooth. To keep the sample clean it is important to keep any dust or debris from getting on the sample. Once the sample has been irradiated it is not possible to clean the sample with solvents because of contamination of any radioactive material in the waste solvent, so it is important to try to keep the sample as clean as possible. In the gamma irradiations, it has been found that

the germanium layer becomes rough after a dose of greater than 12 Mrad. This makes the MOKE signal more difficult to resolve.

Chapter 6: Experimental Results

6.1 Introduction

There are two experiments performed on these samples. One is a gamma irradiation experiment, and the other is a neutron experiment. The former will be discussed in this section and the later will be the topic of next section. We performed the gamma irradiation first because the reactor produces both gamma rays and neutrons, which makes it important to understand the effects that gamma rays have on our samples over time so that we can distinguish gamma effects from neutron effects.

6.2 Gamma Irradiation Experimental Results

The samples for this experiment were gamma irradiated over a period of 28 days of exposure. Five samples were irradiated, 3 field grown, 2 field cooled. As mentioned above the samples were composed of SiO₂ substrate/10nm Py/6.1nm Cu/10nm Py/20nm FeMn/10nm Ge. The two field cooled samples were 2mm by 5mm. Field grown samples 1 and 3 were 2mm by 5mm, but field grown sample 2 was 1mm by 5mm.

The samples were all irradiated at the same time in the gamma irradiator. They were taken out several times during this process to be characterized. There were also two control samples that were never irradiated, but were measured whenever we measured the irradiated samples. They were taken out after a total exposure of 1, 2, 3, 5, 7, 11, 17.5, 25, 28 days. This was to look for any behavioral trends that may have occurred during

the exposure time. As discussed above we characterized the samples using MR, MOKE, and VSM. MR, and MOKE were both taken simultaneously. Though the signal from the samples became noisier as the exposure time increased, it was still possible to extract exchange bias, coercivity, and MR from all of the samples except field grown sample 2, which could no longer be measured after 17.5 days, which corresponds to 30Mrad of exposure.

Exchange Bias

The exchange bias data is shown for the VSM, MR, and MOKE measurements in Figure 17 below. Notice first of all that the three measurements show the same trend. This tells us the trend we see is real, and that either of these characterization techniques can give us insights into this trend. It does not come as a surprise at all that the exchange bias is hard to gamma radiation, because as mentioned earlier, we would expect that electron displacements caused by gamma rays would cause negligible, if any effect in metals, since electrons are free to move around. Notice that the VSM exchange bias is slightly lower than the exchange bias from the MR/MOKE measurements. This is likely due to both a difference in calibration of the gaussmeters that measure the field in the two magnets, and a small angular offset that is inherent in the VSM measurement.

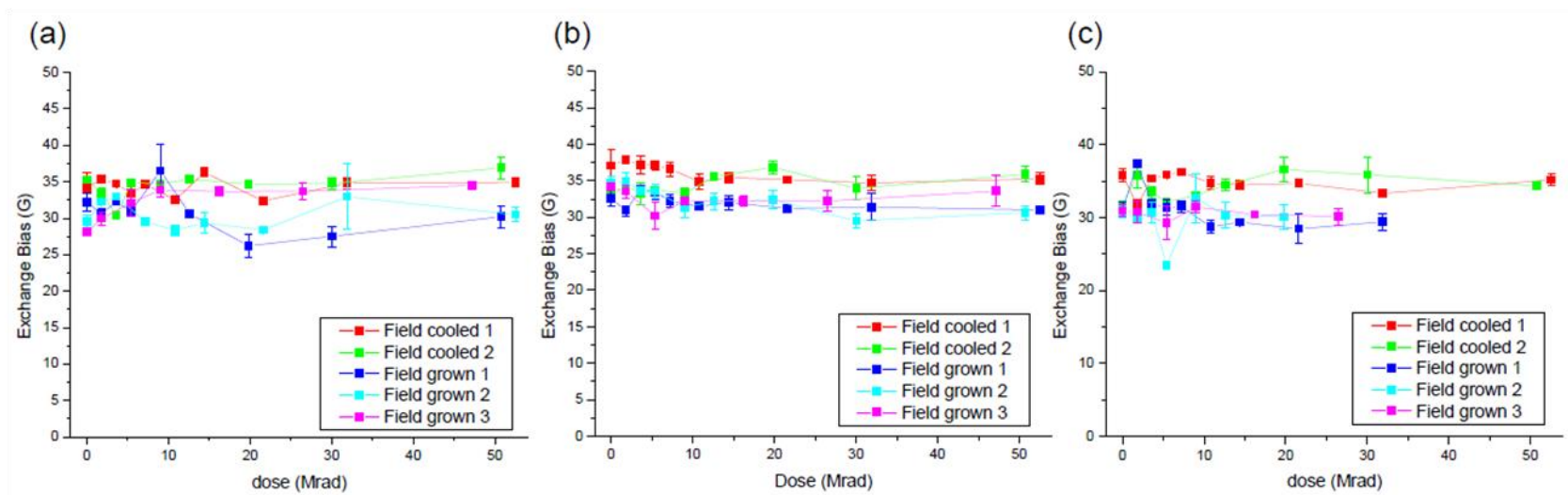


Figure 17: Graph of exchange bias vs. dose for field cooled and field grown samples from the (a) VSM measurement. (b) MR measurement. (c) MOKE measurement. All three graphs show there is no change in the exchange bias of the sample with the gamma irradiation of the samples.

Coercivity

Figure 18 shows the coercivity vs. dose for the VSM, MR and MOKE measurements. This data shows a dramatic, yet unpredictable shift in coercivity. We can see that the change in coercivity is somehow linked to the irradiation because the control samples show no changes in coercivity over the same time period. This is a bit of shocking because we saw no change in exchange bias, yet there is this erratic behavior with the coercivity. As mentioned above though, exchange bias is partially responsible for the increase in coercivity that we see in the exchange biased layer (though it is definitely not the only factor impacting the coercivity). Therefore, if we see no change in exchange bias, it would be fairly reasonable to expect to see no change in coercivity.

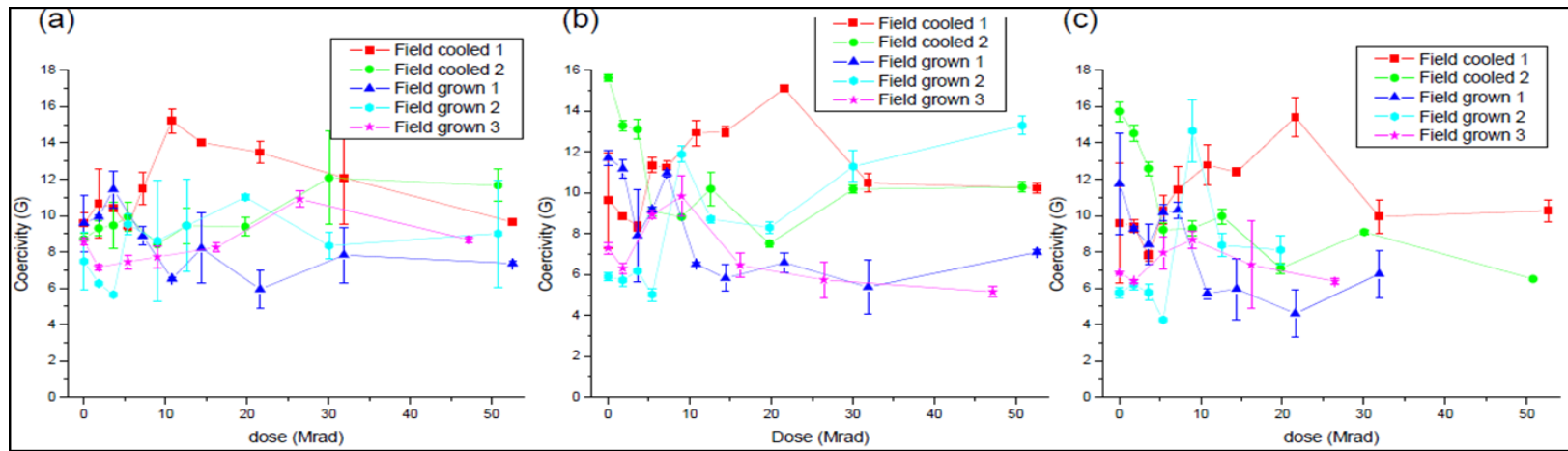


Figure 18: Graph of coercivity vs. dose for field cooled and field grown samples from the (a) VSM measurement. (b) MR measurement. (c) MOKE measurement. All three graphs show a nonmonotonic change in coercivity with the gamma irradiation of the samples.

Magnetoresistance

In Figure 19, we see plots of MR ratio vs. dose. Notice that as mentioned above, the field cooled samples has a higher MR than the field grown samples. This data also shows a monotonic decrease in MR. The overall decrease in MR for a given sample is anywhere from 0.15% to 0.44%. Just as with the coercivity data, comparison of the irradiated samples to the non- irradiated samples makes it clear that the decrease in MR is in some way linked with the irradiation.

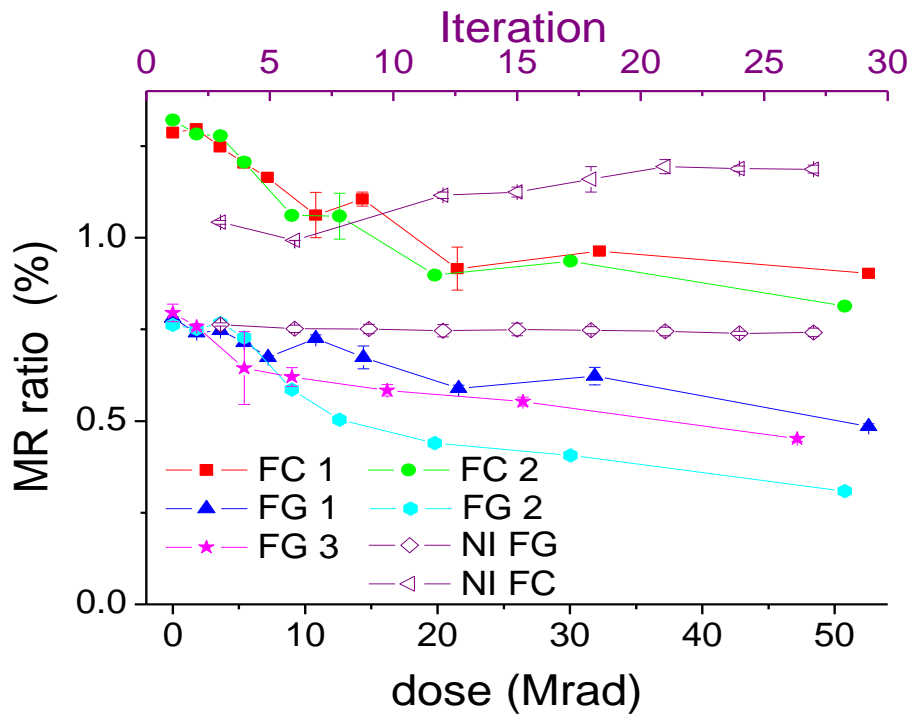


Figure 19: Graph of MR ratio vs. dose for field cooled and field grown samples from the. The MR decreases with increasing exposure time.

Microscopy on Samples

The gamma radiation study yielded the following results: no change in exchange bias, no monotonic change in coercivity, and a steady decrease in MR ratio among the samples that were irradiated. The changes in coercivity and MR were counter to what we expected so we decided to perform microscopy on the samples in attempt to make sense of what was going on.

Figure 20 shows SEM images on two different locations on one of the samples. Figure 20a is an SEM image of a part of the sample that was exposed to air during the irradiation. Notice the surface deformation and damage on this part of the sample. Figure 20b is a cross section of the same area, and more explicitly shows that the cracks go through the magnetic layers of the sample. Figures 20c and 20d, which are an SEM image and FIB cross section taken under one of the indium contacts. Interestingly there is no deformation, or cracking under the indium.

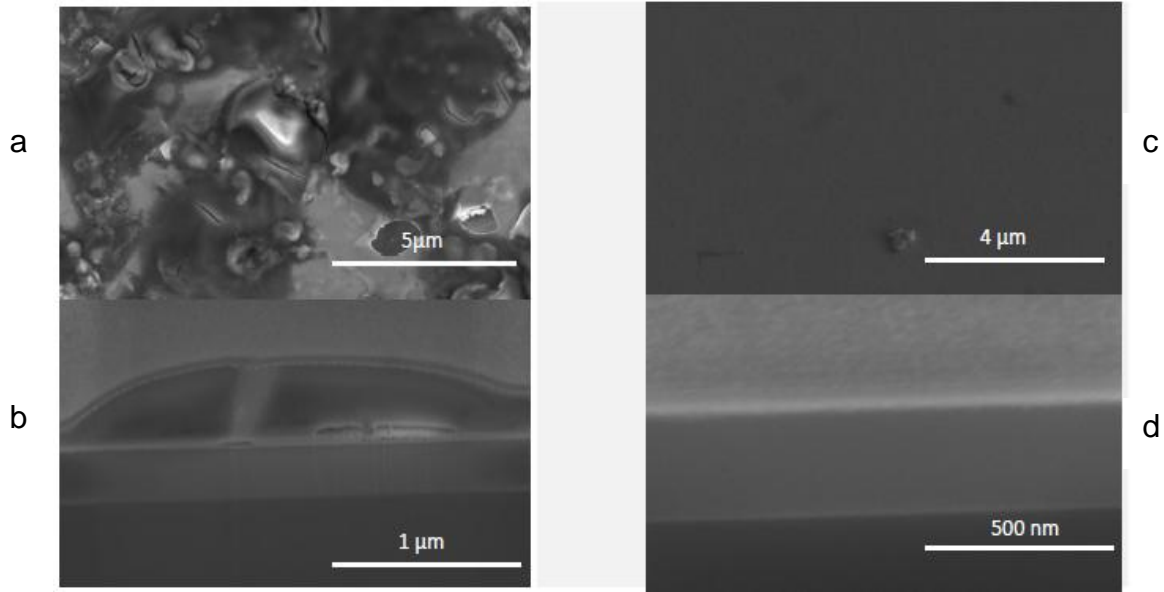


Figure 20: (a) SEM image of an area of one of the samples that was unprotected during the gamma irradiations. (b) FIB cross section of the same location. (c) SEM image of an area of the sample that was covered with indium. (d) FIB cross section of the same indium covered areas.

It seems that there are two effects at work here, neither of which arise directly from the gamma ray exposure. First, it appears that the cracks and delamination are due to oxidation of the Ge capping layer. This layer is intended to protect the FeMn layer, but we believe that the gamma rays create free charge in the Ge, which dramatically accelerates the oxidation process. This is consistent with the fact that no structural damage occurs under the indium contacts. This suggests that by capping the sample it may be possible to protect the Ge layer from oxidation.

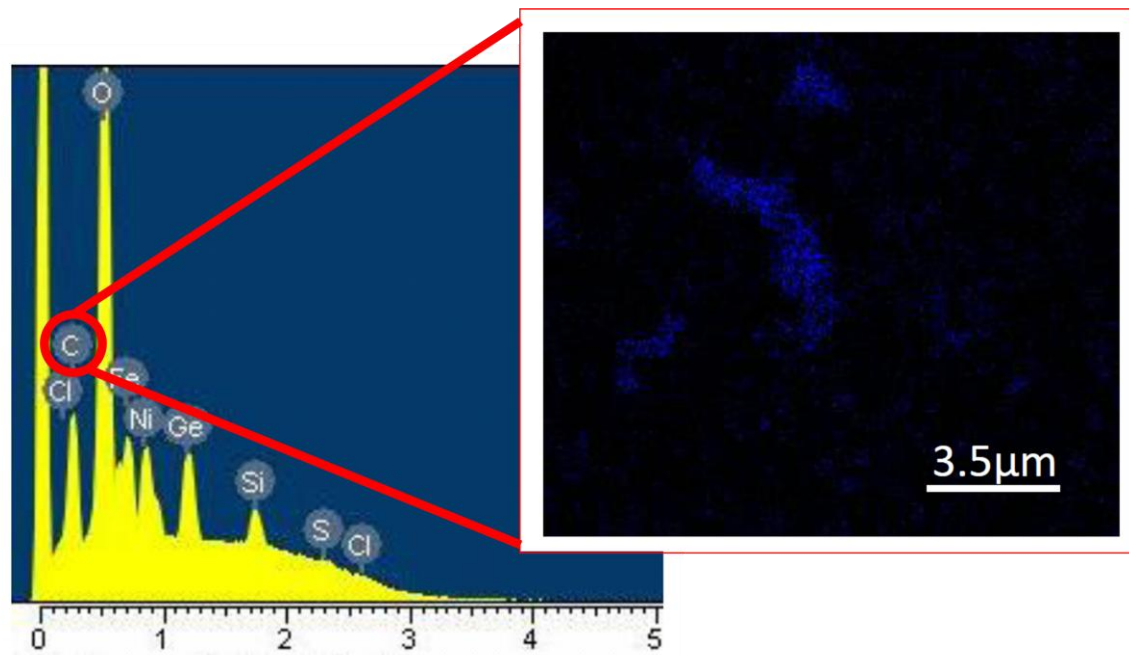


Figure 21: EDS spectrum of the sample imaged in previous figure. We see carbon was deposited during gamma irradiation.

In order to see the second effect at work, we took energy dispersive x-ray spectroscopy (EDS) data on the sample that had been irradiated, shown in Figure 21. Notice that the EDS data shows a carbon peak. Also shown, is a spatial distribution of the carbon on the area of the sample from which the peak is taken. This implies that something during the irradiation caused carbon to deposit onto the samples. The only carbon source of carbon that existed in our setup was the fluoroware containers we kept the samples in during the irradiations. This suggests that the carbon was deposited from the fluoroware that the samples were irradiated in. These containers age, and brown over the exposure period. Fixing this issue should be merely an issue of changing to some non-plastic, and hopefully more stable container.

Once this study was complete several issues remained. First how can we prevent oxidation the Ge layer? This is important, because the data suggests that if the Ge layer is destroyed this causes not only physical damage to the sample, it also effects properties of the spin transport. The next question that needed to be answered was how can we prevent carbon deposition during gamma exposure? As mentioned above this should just be an issue of irradiating the samples in a different container.

A followup study was conducted in which we addressed these issues. In this study we took several measures to ensure that the samples were not damaged by the containers in which they were held, or by surrounding oxygen. In order to do this, we replaced the fluoroware with pyrex vials, and filled the vials with nitrogen gas. The experiment was performed on three samples, all of which were field grown and one was capped with PMMA to see if it would add more protection than just having the sample uncovered in the nitrogen environment. We sealed the vials off with ground glass caps wrapped in Teflon tape. This was to ensure that we could unseal the containers when to do characterization after exposures. We also redesigned the sample, by changing the thickness of several layers of the sample as shown in Figure 22. This was done in hopes of increasing MR ratio to reduce noise issues that may arise in the measurement.

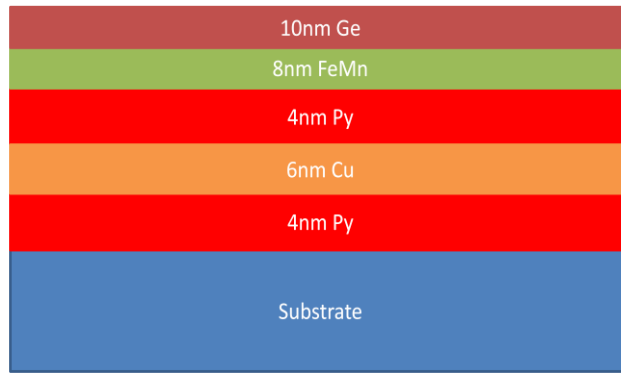


Figure 22: New sample structure used for the followup gamma irradiation study.

Figure 23 shows the MR data for one of the uncapped samples from this study. All of the uncapped samples had their MR completely destroyed after just two days of irradiation. The PMMA capped sample showed the same behavior, but lasted four days. Just as in the previous study the damage is consistent with browning of the container, which this time happened at a much accelerated rate, and with surface damage on the sample that shows up in SEM images Figure 24.

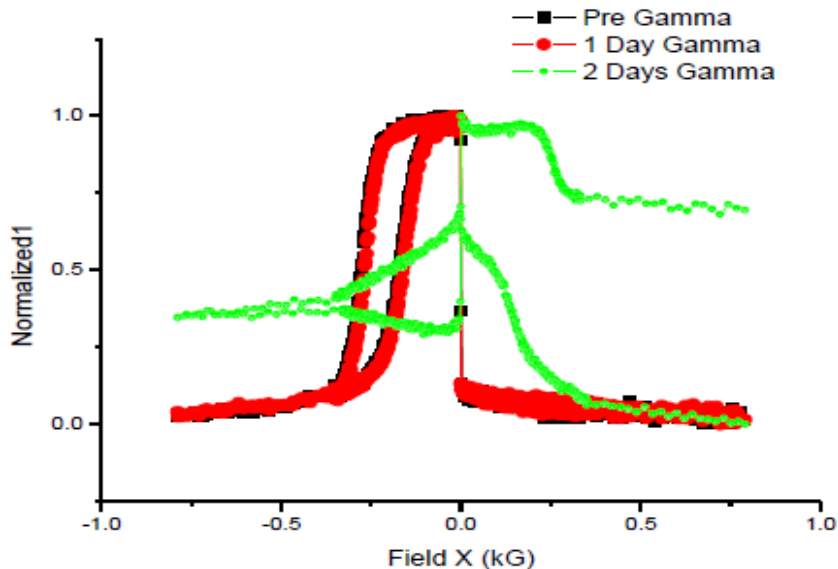


Figure 23: MR results for the followup experiment. MR completely gone after just 2 days of exposure

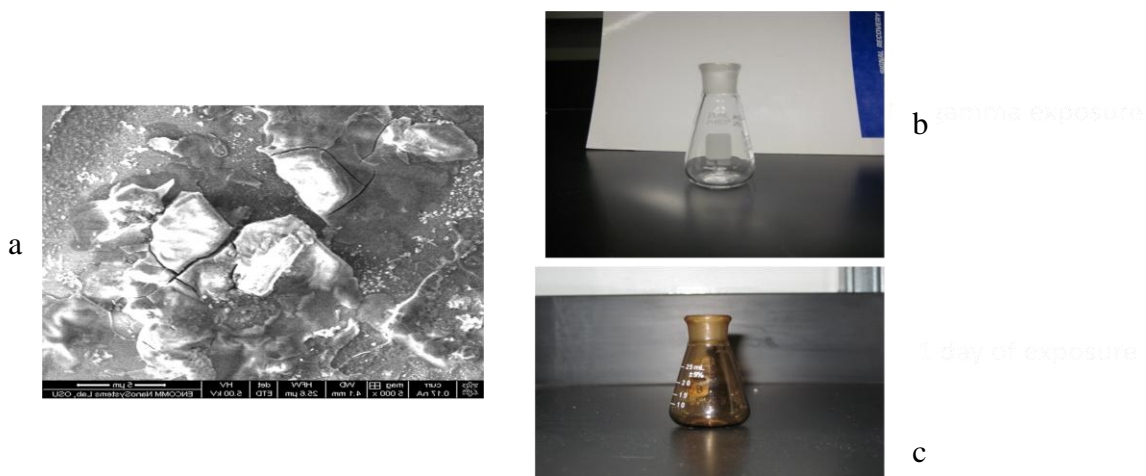


Figure 24: (a) SEM images of the sample after 2 days of exposure show the same surface damage it took a month to see in the previous study. (b) Before irradiation the glass vials in which the samples were irradiated were clear. (c) After 1 day of exposure, there is a very strong browning and aging effect that takes place.

6.2.1 Conclusions for Gamma Radiation Experiment

GMR spin valves appear to be hard to gamma radiation. When they are gamma irradiated, they are still able to hold a well defined MR, coercivity, and exchange bias, all important parameters for a spin valve if it is to be used for applications. There are however there were several effects that caused variations in the MR and coercivity. These issues were oxidation of the Ge capping layer, and carbon contamination of the samples. A follow up experiment was performed to address these issues, by changing the container of the sample, and removing oxygen from the container. When this was performed, however the effects that we saw in the one month gamma exposure happened at a much accelerated rate, 2 days. This follow up experiment should be modified in several ways to ensure the integrity of the samples.

For one thing the browning of the glass happened at a much accelerated rate compared to the fluoroware. It would be worthwhile to look into other containers that perhaps have been used in gamma irradiation studies before, to find one that will allow us to complete this study without worry of this effect. Secondly it is possible that the vials were not as air tight as we thought they were so that oxidation occurred. This is an unlikely explanation for the acceleration of the damage though, because when the samples were in fluoroware they were completely surrounded by oxygen.

6.3 Neutron Radiation Experimental Results

For the neutron irradiation only one sample was measured. It was a field grown sample that had dimensions of 2.5mm by 5mm. the sample had three exposures, each

with a dose of total neutron flux of 6×10^{12} nv and a fast neutron ($E > 0.5\text{MeV}$) flux of 1.4×10^{12} nv.

Once the sample was neutron irradiated, the indium contacts become radioactive which prevented us from performing VSM measurements on the samples. Because of this, we can only take MR and MOKE data on this sample.

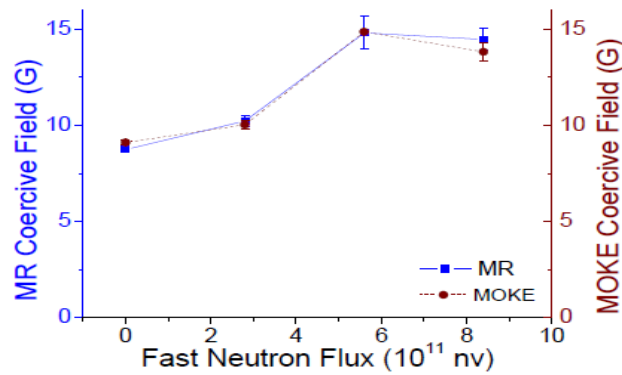


Figure 25: Graph of the coercivity vs. fast neutron flux for both the MR and MOKE measurements. The blue line is the MR measurement and the brown line is the MOKE measurement.

Figure 25 shows the coercivity vs fast neutron flux for both the MR and MOKE measurements. Though it appears that the coercivity is steadily increasing, we believe that the sharp changes seen in the coercivity are once again non-uniform variations in the coercivity with respect to dose. Figure 26 shows the exchange bias vs. dose for MOKE and MR. Just as with the 1 month gamma irradiation experiment, there is no variation in the exchange bias of the sample. Figure 27 shows MR vs fast neutron flux for the sample. Here there is no change in MR at all, which is different from the result seen in the gamma irradiation experiment.

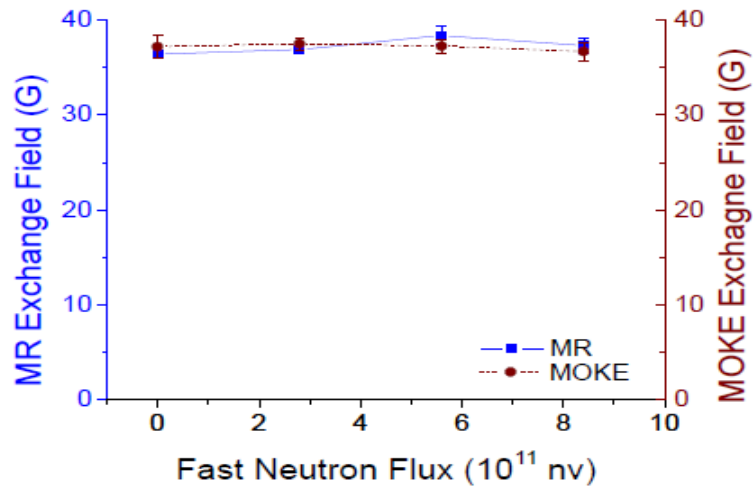


Figure 26: Graph of the exchange bias vs. fast neutron flux for both the MR and MOKE measurements. The blue line is the MR measurement and the brown line is the MOKE measurement.

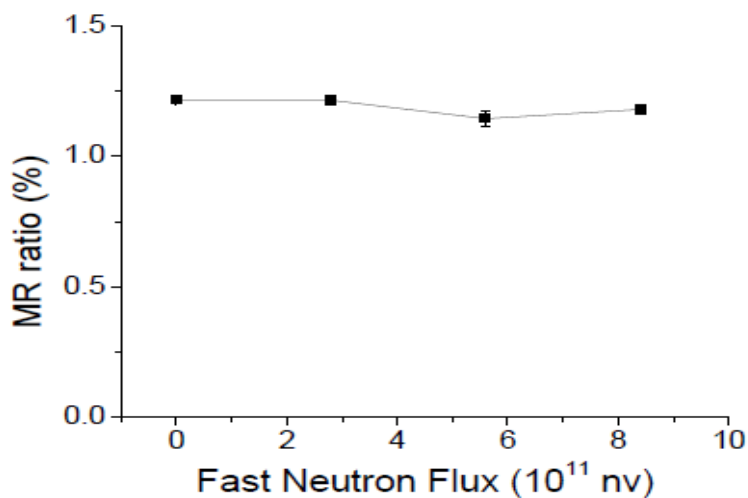


Figure 27: Graph of the MR Ratio vs. fast neutron flux.

6.3.1 Future Directions for the Neutron Radiation Experiment

The samples are hard to the amount of radiation exposure that was given to them. This seems strange, because as described earlier in this thesis, it would seem the atomic displacements caused by neutrons would cause fairly heavy amounts of damage in our samples. One possible explanation for why there is no damage observed, is that there is a room temperature annealing effect that takes place. In other words it is possible that the interstitials are not knocked very far from their respective vacancies and are able to return to them over a relatively short period of time at room temperature. There are two ways to modify this experiment to test this hypothesis. First run the experiment at low temperature, second irradiate at higher power.

An experiment is currently being set up to address these two issues. We have designed a low temperature system in which we can perform the experiment, Figure 28. Originally we used a glass Dewar for this experiment, however when we irradiated the Dewar, it browned heavily and broke. We have since replaced that Dewar with a foam Dewar made by Spear Labs. The dewar has a 2 liter volume, a 5.6 inch diameter, and a life of roughly 8 hours at room temperature. The platform is designed to place the sample exactly 15'' off the ground, which ensures that the samples see the maximum dose of radiation possible. To protect the sample from thermal neutrons, the apparatus will be wrapped in cadmium before it is irradiated. In order to monitor the temperature in the Dewar throughout the irradiation to ensure that the liquid nitrogen has not boiled off, a thermocouple will be placed inside the Dewar, and in order to accommodate for this, there is a hole milled into the top of the Dewar cap, and slots will be cut into the cadmium shield. The platform was fabricated out of 6061 aluminum, because this particular alloy is cheap, easily accessible, and does not produce any really harmful isotopes during irradiation. This makes it an attractive candidate for a metal to use for such an apparatus.



Figure 28: Low Temperature system for the neutron experiment.

This apparatus can fit several samples at once comfortably, and since the materials are fairly heavy, the samples sink right to the bottom even in the presence of LN_2 . We intend to run this experiment at full power, 450kW for 4 hours. The hope is that if the above hypothesis is true, and the reason we see no damage is because of room temperature annealing, then perhaps at cryogenic temperatures this annealing will either not occur, or occur so slowly that we will see damage in our post characterization of the samples. Increasing the power from 100kW to 450kW is another way to probe the effects more strenuously. If the part in the above hypothesis about the atoms not being knocked very far from their vacancies is true, then increasing the power by a factor of 4.5 should knock the atoms a lot farther from their vacancies, which would in turn cause more permanent damage if the neutron irradiation were in fact causing damage to the samples.

If damage is occurring during the neutron irradiations, it would be interesting to observe this damage as it happens, even if we can see its effects afterwards. This may give us insights to several things: whether or not there is any damage occurring, if damage is occurring, how fast the annealing process takes place, whether or not it is possible to slow or halt annealing. In order to try to gather in situ information about the transport, we are currently designing an electromagnet to take MR measurements on a sample while it is being irradiated in the reactor. While the design is not yet finalized, the electromagnet would be a solenoid, with a 1.5'' diameter and the ability to reach a field of at least 400G. This would ensure that we could reach the maximum fields we have need to reach to properly characterize the samples we use for this experiment. It would also have to have a sample stick inside with a height that puts the sample centered at 15'' above the ground so that the sample sees the maximum dose during the irradiation. Also, the electromagnet's core will have to be fabricated out of 6061 aluminum, for reasons described above.

References

1. Binasch, G., Grünberg, P., Saurenbach, F. & Zinn, W. Enhanced magnetoresistance in layered magnetic structures with antiferromagnetic interlayer exchange. *Physical Review B* 39, 4828 (1989).
2. Baibich, M. N. *et al.* Giant Magnetoresistance of (001)Fe/(001)Cr Magnetic Superlattices. *Physical Review Letters* 61, 2472 (1988).
3. The Discovery of Giant Magnetoresistance. *Class for Physics on the Royal Swedish Academy of Sciences, Scientific Background on the Nobel Prize in Physics 2007* (2009).
4. Wolf, S.A. *et al.* Spintronics: A Spin-Based Electronics Vision for the Future. *Science Magazine* Vol. 94 (2001).
5. Tsymbal, E.Y., Pettifor D. G. Perspectives of Giant Magnetoresistance. *Solid State Physics*, ed. by H. Ehrenreich and F. Spaepen, Vol. 56 (Academic Press, 2001) pp.113-237
6. Meiklejohn, W. H.; Bean, C. P. (1957-02-03). "New Magnetic Anisotropy". *Physical Review* **105** (3): 904–913. doi:10.1103/PhysRev.105.904
7. Nogués, J.; Ivan K. Schuller (1999-02-15). "Exchange bias". *Journal of Magnetism and Magnetic Materials* **192** (2): 203–232. doi:10.1016/S0304-8853(98)00266-2
8. Kiwi, Miguel (2001-09). "Exchange bias theory". *Journal of Magnetism and Magnetic Materials* **234** (3): 584–595. doi:10.1016/S0304-8853(01)00421-8
9. Exchange Bias. http://en.wikipedia.org/wiki/Exchange_bias , 2009.
Thompson, M. W. *Defects and Radiation Damage in Metals*. (The University Press, 1969).
10. Parks, S.C. Magnetoresistance and Magnetodynamics in Thin-Film Magnetic Heterostructures. The Ohio State University 2009.
11. Was, G. S. *Fundamentals of Radiation Material Science*. (Springer, 2007).
12. Olander, D. R. *Fundamental Aspects of Nuclear Reactor Fuel Elements*. Vol. TID-26711-P1 (The Department of Energy, 1976).
13. Neel, L. *Ann. Phys.* 2, 61 (1967).
14. *The Ohio State Nuclear Reactor Laboratory*, <<http://www-nrl.eng.ohio-state.edu/>> (2009).
15. Co-60 Decay Scheme. http://commons.wikimedia.org/wiki/File:Cobalt-60_Decay_Schemep.svg , 2010

Appendix A: GMR/MOKE Measurement Instructions

before starting, make sure laser is warmed up, at least two hours...plan ahead

1. Get Sample and the sample mount
 - a. Sample can be obtained by asking the individual in charge of the project or where they have specified retrieval.
 - b. Make sure the sample is ONLY handled while wearing latex-ish gloves.
 - c. The mount might be out on the desk near the computer just inside the door or in place between the two electromagnets

NOTE: If sample is irradiated make sure to use only tools designated for such (and be sure you are certified handle).

2. Install wire on indium contacts – SKIP THIS STEP IF ONLY DOING MOKE MEASUREMENT

- a. Place sample on a glass slide found at the end of the table island within the storage unit in the drawer labeled “glass slides”
 1. Make sure the shiny side of the sample is facing up toward you.
- b. Retrieve the indium wire at the same unit in drawer “Indium Wire”
- c. Grab a razor blade (usually on top of unit)
- d. Cut a thin (fingernail thickness-ish) full slice of wire and place on glass slide

1. Chop this sliced piece of indium into four quarters (four pie pieces)
- e. Get a wooden cotton swab and wrap end with Teflon tape (white looking plumbers tape) you will only need 2 or so inches of tape.
1. You will use this wrapped end to move indium to the sample and the sample mount
- f. Grab two 1½ (ish) cuts of ultra fine wire, usually found on top of the unit, and get ready to put one wire on one end of the sample and then on the other
- g. Move a ¼ piece of indium, using the wrapped stick end, to one edge of the sample and place one piece the ultra fine wire end in-between the installed indium and the indium hanging onto the sample mount. Squish the wire in-between the two indiums. BE GENTLE
- h. Repeat for other side of sample until sample looks like this

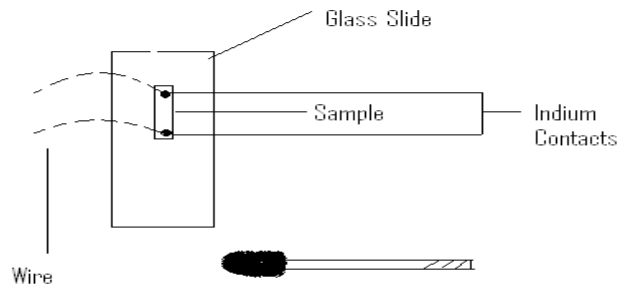


Figure 29: Pasting Sample onto Sample stick and attaching indium press contacts.

3. Get Rubber Cement out (top of unit)
4. Place sample onto the sample mount using the rubber cement
 - a. Sample will be best if near the middle of the sample mount and lengthwise parallel to the mount
 - b. use back of a wooden toothpick to slop the glue onto the MOUNT
 - c. using tweezers gently move sample to the glued area
 1. be sure to have the shiny side up
 - d. press sample flat only on the indium contacts KEEP shiny side free of everything
5. Wire sample to mount SKIP THIS STEP IF ONLY DOING MOKE

a. Using the two remaining indium pie quarters and technique above mentioned install wires onto the mount on the desired connection (not to the same line)

1. These connections are in pairs as shown below 1&2 3&4 etc.

2. Make sure that all wires are out of the way of the laser beam

b. Sample glued on and all wired up should look like this:

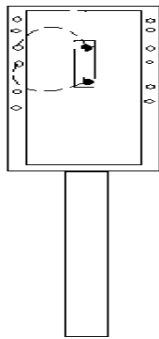


Figure 30: Sample wired on the stick.

6. Place mount in holster between magnets **BE AWARE OF THIN WIRING COMING OFF OF THE MAGNET. DON'T BUMP IT OR MESS WITH IT AT ALL.**

- a. Plug in sample mount. Female connection is located behind mount holster.
Make sure there is a “seatbelt” click to ensure proper connection.
- b. Before tightening down mount into holster ensure mount is perpendicular to magnet heads like so:

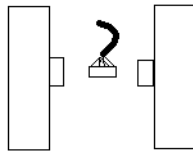


Figure 31: Sample inside magnet.

7. Follow steps to make sure equipment is all connected and working

a. GMR

1. Now that the sample is installed do some eyeball checking

- i. Make sure there are no loose wires or debris around the experiment area
- ii. Check that the water that cools the magnet is turned on by feeling hose for vibration.
- iii. Check and connect all cables

- a. Thick grey cable next to where sample cable was connected should be connected into the green unit on the tower labeled “4 Point Measurements” as shown below
- b. 2nd cable on the green unit should be connected to the corresponding connections you made when connecting the sample to the mount (ie 1&2 or 3&4 etc.)

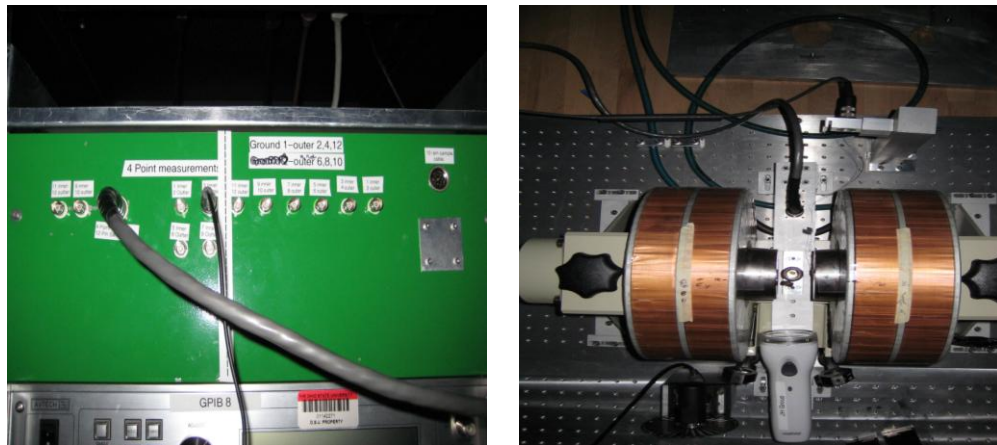


Figure 32: GMR setup and breakout box.

- i. That small black cable will come from the small silver box on the tower. The other end of which will be plugged into the GPIB 13 on the left side in space 'A'. See Picture below

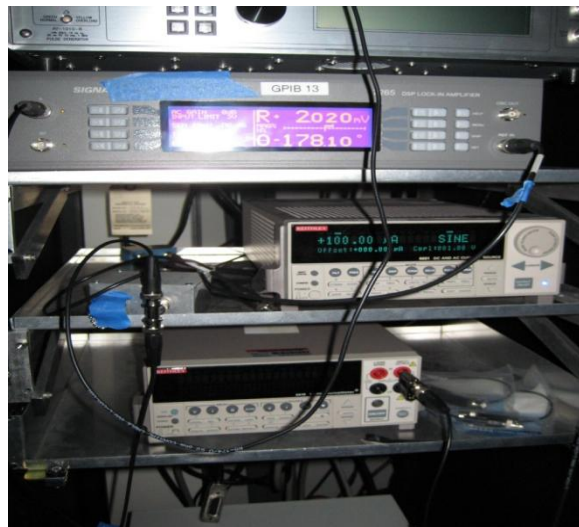


Figure 33: GMR Electronics.

8. Now make sure all equipment for GMR is on
 - iv. Lock-in GPIB 13 pic shows device is on

- v. The bottom Kepco power supply (flip switch up to on – picture shows the Kepco is off) Make sure sample is in before this step
- vi. See pictures for equipment recognition (as well above)



Figure 34: Kepco power supply and GMR lockin.

b. Moke

1. Turn on warmed up lazer and direct beam toward sample
 - i. Get beam to lie directly on the surface (preferably in the middle) of the sample.
 - a. Note: lenses not on the lazer or photo eye mount should be down until later step.

2. Tighten down the laser mount to the table with the provided allen wrench
3. Where the beam is reflected use the photo electric eye or photo eye to “capture” the end of the beam.
 - i. Make sure that the beam is precisely in the middle of the photo eye so as to get the proper measurements.
 - ii. Tighten down the photo eye mount to the table
4. Now go to the two lenses near the magnet (they were put down earlier)
 - i. Pull up the first lens and adjust left/right (left lens) to get beam to shine through it near its middle.
 - a. You want the beam to be securely on the sample as well. As close to where the beam was before inserting the lens.
 - b. Tighten the lens making sure that the beam is where it should be.
 - ii. Pull up the second lens and follow same steps only this time make sure the beam is located directly on the photo eye.
 - a. NOTE: do not move the laser or the photo eye!
 - b. Tighten the lens and make sure beam is where it should be
 - iii. See “drawing” for desired result and look and pics.

- iv. Check for stray beams and contain them

Desired Result & Look

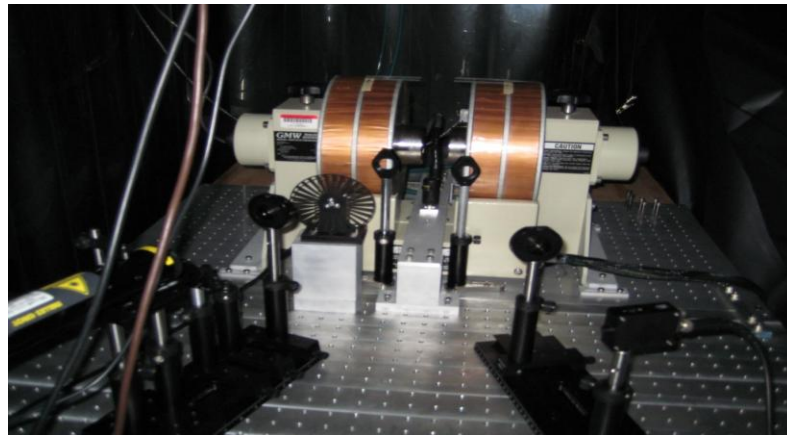
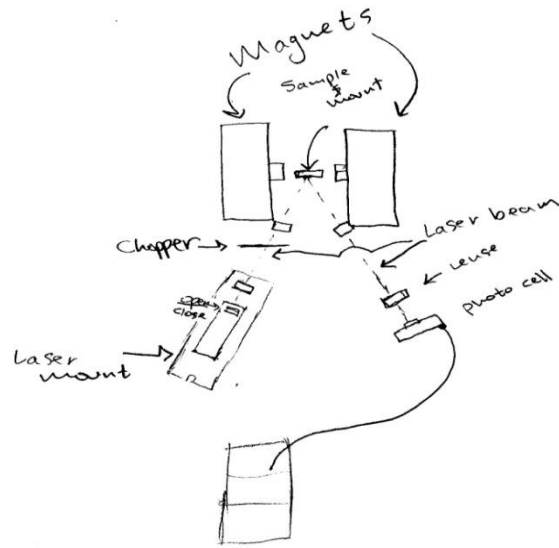


Figure 35: Schematic, and picture of MOKE setup.

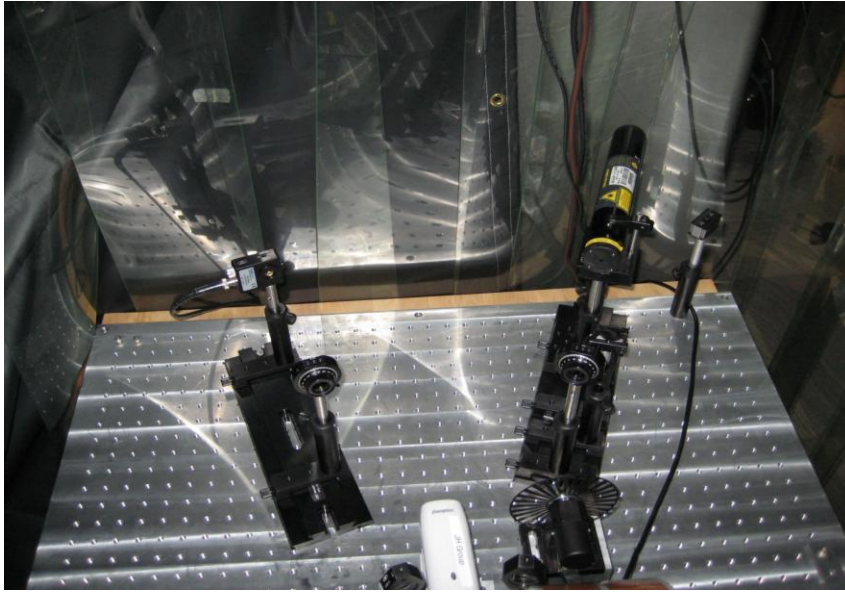


Figure 36: Laser and Polarizers on MOKE setup

5. Turn on “chopper” at tower next to the laser on device labeled: “Thor” with the button “ext in enable”
 - i. The chopper should be set to 3000 rpms (wait a couple min for it to get up to speed.
6. Turn on the device labeled: “SR570”
7. Make sure that they are connected to their corresponding machines
 - i. Thor to hook up to lock-in GPIB 7 on the right side on connection ‘ref in’ (as pictured)
 - ii. SR570 to GPIB 7 on the left side on connection ‘A’
 - iii. Make sure GPIB address is set to 7

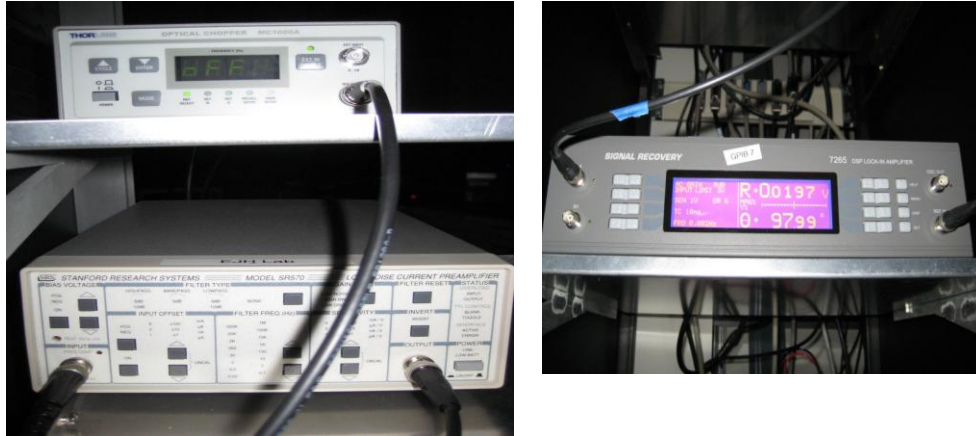


Figure 37: MOKE electronics.

8. Now that all the equipment is hooked up and ready to go head over to the computer and open “Labview” program GMR_MOKE_lockin_v5b_3.vi
 - a. On the settings page you will see a button just below the ‘view’ tab that is an arrow pointing to the right. With all the equipment on and set up click that arrow to begin the measurements.

Appendix B: Data Analysis for GMR in Origin 8

NOTE: For simplicity, assume we are analyzing **pre-radiation** data for the sample **B588b**.

(1) Pre-Analysis Organization

1. Open Origin 8.
2. Right-click on the folder “Folder1” under “UNTITLED” and select “New Folder”.
3. Go to File\Save Project. Save the project in the following location: \\phypcs\jh group\Group Projects\radiation Project\data\B588\B588b. Save the project as “B588b”.

Once it is saved, the name “UNTITLED” becomes “B588b”.

4. Right-click on “Folder1” and select Rename. Call it “GMR\MOKE”. This is where all of the GMR\MOKE data will be stored for B588b.
5. Right-click on “Folder” and select Rename. Call it “pre_rad”. This is where all of the pre-radiation data will be stored for B588b.

6. While “pre_rad” is selected, go to File\New and double-click on Workbook. This creates a blank workbook in the selected folder. The default title will be “Book2”.

7. Under My Computer, go to \\phypcs\jh_group\Group Projects\radiation Project\data\B588\B588b. Open the folder named after the date that contains “Run1”. Open the folder “Run1”. There are two text documents: “Curve” and “Parameters”.

8. Drag “Curve” into “Book2”. This transfers all the data into the workbook, and changes the name of the workbook as shown in the left-bottom screen from “Book2” to “Curve.txt”. Right-click on “Curve.txt” and select Rename. Call it “Run1_date”. The date should be written in the format day month year (e.g. 19may10).

9. In the first column “A(X)”, double-click on the cell in the row “Comments” and type in the date of the run in the same format. After the last column, right-click in the empty gray space and select Add New Column. The default title is “D(Y)”.

10. Click on the title of the new column “D(Y)”. This will select the entire column.

Right-click on the column and select Set Column Values. This opens a window

where you can type in a formula. Paste in the following formula:

$(\text{col(B)}+\text{col(C3)}+\text{col(C6)}+\text{col(C9)}+\text{col(C12)}+\text{col(C15)}+\text{col(C18)}+\text{col(C21)}+\text{col(C24)}+\text{col(C27)})/10.$

Click OK. This formula computes the average value of dV/dI in ohms for 10 cycles, for each field value. (The negative sign is to correct the intrinsic minus sign in the program.) Note that this formula is based on the default names for each column, and may need adjustment if the names change or if the cycle number is different from ten.

11. Click on the title “D(Y)”. Right-click on the column and select Normalize. Leave the settings as Manual and click OK. This will normalize the values to [0,1] and output the values to a new column (it will make a new column after the last column D(Y)). The default title of the new column is “C(Y)”.

12. Click on the title “D(Y)”. On the tool bar underneath the main working space, the third icon from the left is a slanted line with three dots on it. Click on this icon while the column “D(Y)” is selected. It will create a graph of the data, with default title “Graph1”. Right-click on “Graph1” in the left-bottom screen and select Rename. Call it “Run1_date”.

Now we will begin the actual data analysis.

(2) Find the MR ratio for “Run1”

1. Click on the title “Curve”. Right-click on “Curve” and select Add. This will create a new sheet after “Curve”. The default name is “Sheet1”. Right-click on “Sheet1” and select Rename. Call it “FinalNumbers”. Copy and paste the template of “FinalNumbers” from the document located at
`\\phypcs\jh_group\Group Projects\radiation Project\data\GMR_organization sample.`
2. On the graph “Run1” find the tail of the ferromagnetic loop. The points in the FM tail should have the lowest dV/dI values of the entire graph. Assume that the tail is on the left side of the graph. Click on the title “Curve” to pull the sheet of raw data to the foreground. Look at column “A(X)” for the field values, and record the interval of rows in which the 50 lowest field values occur. These are the 50 furthest left points on the graph in the FM tail.
3. In the column “D(Y)”, highlight the 50 values in this interval of rows.
IMPORTANT: To select a string of data, click on the first value you want to include and scroll the mouse until the pointer rests on the last value you want to include. To select multiple strings of data at once, select the first string as above, and before beginning the second string hold down the Control key on the

keyboard. As long as the Control key is held down when you click the mouse to create a new string, all of the previous strings will remain selected.

(If the FM tail is on the right side of the graph, record the interval of rows in which the 50 highest field values occur, and highlight these 50 values in “D(Y)”.)

4. Right-click on the highlighted data and select Statistics on Column\Open Dialog. Under Input Data select ‘Combined as Single Dataset’ and click OK. This creates a new sheet in the workbook “Run1_date”. The default name is “DescStatsOnCols1”. From this we can read off the mean value of the resistance at the base, which we call Rbase. Put it in the appropriate column in the sheet “FinalNumbers”, “J(Y)”.
5. In the column “C(Y)”, which contains the normalized values, find the two peaks. You can easily see where they should occur if you use the normalized values. From the Sparklines graph, you can see which peak occurs first: the large peak (which has a thicker width) or the small peak (which has a thinner width).
6. Highlight 20 points after the vertical jump occurs for the first peak, and then hold down Control and highlight 20 points after the vertical jump occurs for the second peak.

7. Right-click on the highlighted data and select Statistics on Column\Open Dialog. Under Input Data select 'Independent Columns' and click OK. This creates a new sheet in the workbook "Run1_date". The default name is "DescStatsOnCols2". This sheet lists the statistics for the first group you highlighted in the first row and the statistics for the second group in the second row.

8. In order to make things clear, double click the title of the first row in the sheet "DescStatsOnCols2". It will have the default name "D (1)". Rename it either: (i) "lar\", if it is the large peak, or (ii) "sm\", if it is the small peak. Look at the graph "Run1_date". After the "\ " in the row title, type either: (i) "lo", if the peak occurs at low field, or (ii) "hi", if the peak occurs at high field. After you rename "D (1)", the new title for "D (2)" is obvious (e.g. if "D (1)" becomes "sm\hi" then "D (2)" has to be "lar\lo"). From this we can read off the mean value of the resistance at the two peaks, both $R_{\text{peak large}}$ and $R_{\text{peak small}}$. Put them in the appropriate columns in the sheet "FinalNumbers", "K(Y)" and "L(Y)" respectively.

9. The MR ratio= $(R_{\text{peak}}-R_{\text{base}})/R_{\text{base}}$.
 In the sheet "FinalNumbers", click the title "MR ratio large", which is column "H(Y)". Right-click on the column and select Set Column Values. This opens a window where you can type in a formula. Paste in the following formula: $(\text{col}(k)-\text{col}(j))/\text{col}(j)$.

10. In the same sheet, click the title “MR ratio small”, which is column “I(Y)”. Right-click on the column and select Set Column Values. This opens a window where you can type in a formula. Paste in the following formula: $(\text{col}(\mathbf{l})-\text{col}(\mathbf{j}))/\text{col}(\mathbf{j})$.

(3) Find the Coercive Field and Exchange Bias for “Run1”

1. Using the graph “Run1_date”, we associate high with the peak that switches at a higher field value and low with the peak that switches at a lower field value.
2. In the sheet “FinalNumbers”, click the title “High”, which is column “B(Y)”. Right-click on the column and select Set Column Values. This opens a window where you can type in a formula.
 - a. If the high peak is also the **large** peak, paste in the following formula:
 $((\text{col}(\mathbf{k})-\text{col}(\mathbf{j}))/2)+\text{col}(\mathbf{j})$.
 - b. If the high peak is also the **small** peak, paste in the following formula:
 $((\text{col}(\mathbf{l})-\text{col}(\mathbf{j}))/2)+\text{col}(\mathbf{j})$.
3. In the same sheet, click the title “Low”, which is column “D(Y)”. Right-click on the column and select Set Column Values. This opens a window where you can type in a formula.
 - a. If the low peak is also the **large** peak, paste in the following formula:
 $((\text{col}(\mathbf{k})-\text{col}(\mathbf{j}))/2)+\text{col}(\mathbf{j})$.

b. If the low peak is also the **small** peak, paste in the following formula:

$$((\text{col}(\mathbf{I})-\text{col}(\mathbf{j}))/2)+\text{col}(\mathbf{j}).$$

4. Select the graph “Run1_date” in the workspace. On the tool bar on the left side of the screen, select the second icon from the top. This is the Zoom In tool. Zoom in on the area of the graph where the values high and low occur on the y-axis. On the same tool bar, select the fourth icon from the top. This is the Screen Reader tool.
5. Find Field High first. Hover the mouse over the line of the graph that is the furthest right (this is the higher field peak). Click the mouse on this line until the readout for Y is within 0.0005 of the value you computed for High. When this is achieved, record the number for X as Field High.
6. Find Field Low the same way. Hover the mouse over the line of the graph that is the furthest left (this is the lower field peak). Click the mouse on this line until the readout for Y is within 0.0005 of the value you computed for Low. When this is achieved, record the number for X as Field Low. Put Field High and Field Low in the appropriate columns in “FinalNumbers”, “C(Y)” and “E(Y)” respectively.
7. In the sheet “FinalNumbers” click the title “Coercive Field”, which is column “F(Y)”. Right-click on the column and select Set Column Values. This opens a

window where you can type in a formula. Paste in the following formula: $(\text{col}(c) - \text{col}(e))/2$. Click OK.

8. Click the title "Exchange Bias", which is column "G(Y)". Right-click on the column and select Set Column Values. Paste in the following formula: $(\text{col}(c) + \text{col}(e))/2$. Click OK.